J. Fluid Mech. (1999), *vol.* 378, *pp.* 167–196. Printed in the United Kingdom

Structure of Taylor cone-jets: limit of low flow rates

By LEONID T. CHERNEY†

Institute of Mechanics, Moscow State University, Michurinsky prospect 1, Moscow, Russia

(Received 21 January 1997 and in revised form 6 August 1998)

In this paper the structure of the Taylor meniscus and emitted jet is studied by perturbation methods in the limit of low flow rates. An asymptotic system of governing equations is derived from the basic equations of electrohydrodynamics. They rigorously take into account the inertia and viscosity of the liquid as well as the surface ion mobility. The solutions to the asymptotic equations in the meniscus, jet and surrounding gas regions are found, matched with each other, and applied to study distributions of electric and hydrodynamic variables. Such an approach allows the liquid velocity, surface charge, and meniscus-jet radius as well as electric potential inside and outside the liquid to be calculated. We also derive the theoretical dependences of the current carried by the jet and its diameter on the liquid properties and flow rate. These dependences are consistent with the scaling laws found experimentally by Fernández de la Mora & Loscertales (1994) and data obtained by Chen & Pui (1997).

1. Introduction

Stable conical protrusions at the interface between a conducting liquid charged to a sufficiently high electric potential and a gas were first studied by Zeleny (1914, 1917) and theoretically explained by Taylor (1964). These menisci are often called 'Taylor cones' and are usually held at the end of the capillary needle when their equilibrium and stability are investigated (Cloupeau & Prunet-Foch 1990, 1994; Joffre & Cloupeau 1985; Pantano, Gañán-Calvo & Barrero 1994, among others). One of the remarkable features of such menisci is a charged microjet that can stream from the cone apex under certain circumstances. This jet is fairly steady and can be longer than the conical meniscus emitting it, but eventually breaks into a spray of charged droplets. The jet radius may vary from hundreds of micrometres in hydrocarbons (Jones & Thong 1971; Cloupeau & Prunet-Foch 1989) down to fractions of micrometres in highly conducting liquids (Fernández de la Mora 1992; Chen, Pui & Kaufman 1995) and even atomic dimensions in liquid metals (Benasayag & Sudraud 1985; Gabovich 1984). The ratio of jet speed to mean speed in a capillary needle can be as large as 10^7 (Fernández de la Mora 1992).

The phenomenon of the natural formation of Taylor menisci ejecting charged microjets is of greatest practical interest since it is the basis of electrospray atomization of liquids in the so-called cone-jet mode (Cloupeau & Prunet-Foch 1989). This method of atomization is used in fuel injectors and other atomizers (Bailey 1988) and for drug delivery by inhalation (Tang & Gomez 1994). Furthermore, electrospray atomization of liquids in the cone-jet mode is capable of producing monodisperse droplets in

† Correspondence address: 18506-92A Ave, Edmonton, Alberta, Canada, T5T 1V4.

the nanometre size range (Rosell-Llompart & Fernández de la Mora 1994; Chen *et al.* 1995; Lohmann & Schmidt-Ott 1995) and even highly charged gas-phase ions of macromolecules (Fenn *et al.* 1989). These features are of vital importance for new materials production technologies based on ultrafine particles (Gleiter 1989; Gutmanas 1990) and for the mass spectrometry of proteins and other large biological molecules (Fenn *et al.* 1989; Smith *et al.* 1991). Investigation of Taylor menisci and emitted jets is also of significant theoretical interest because their structure often determines important phenomena such as Coulombic explosions of highly charged droplets (Fernández de la Mora 1996; Gomez & Tang 1994).

The state of studies and applications in electrospray atomization has been reviewed in a special issue of *Journal of Aerosol Science*, Vol. 25 (6), 1994. Systematic experimental investigations of the cone-jet mode of electrospray atomization have yielded the following approximate scaling laws for the case of polar liquids with values of the dielectric constant $\epsilon \gtrsim 10$ and electrical conductivity $K \gtrsim 10^{-5}$ S m^{-1} (Fernández de la Mora & Loscertales 1994):

$$I = f_{exp}(\epsilon)\left(\gamma K Q/\epsilon\right)^{1/2}, \tag{1.1}$$

$$R^* \sim r^*, \quad r^* \equiv \left(\epsilon\epsilon_0 Q/K\right)^{1/3}. \tag{1.2a,b}$$

Here Q is the volume flow rate of liquid through the meniscus and emitted jet; I is the current carried by the jet; R^* is the jet radius measured at the jet head, i.e. near the cone apex; ϵ, γ, K are the dielectric constant, surface tension coefficient, and electrical conductivity of the liquid, while ϵ_0 is the electrical permittivity of vacuum. The function $f_{exp}(\epsilon)$ has been measured for a wide variety of non-water and water solutions by Fernández de la Mora & Loscertales (1994). The measurements by Tang & Gomez (1994), Chen & Pui (1997), and Gañán-Calvo, Dávila & Barrero (1997) also confirm equations (1.1), (1.2). The ratio R^*/r^* is a quantity of order of 0.1 which cannot be measured precisely since the meniscus surface continuously turns into the jet surface through some transition region whose boundaries are not defined unequivocally. The quantity r^* can be interpreted as a possible typical dimension of this region.

The most remarkable features of the scaling laws (1.1) and (1.2) are their independence of the liquid viscosity coefficient μ and liquid density ρ. A preliminary explanation for this behaviour has been offered by Fernández de la Mora & Loscertales (1994). They pointed out that parameters ρ and μ become irrelevant quantities in (1.1) and (1.2) if the viscous forces are sufficiently large in comparison with the inertial and capillary ones at the jet head. In this case, the jet velocity profile will be nearly flat and independent of ρ and μ.

Reviews of numerous data and theoretical models for the cone-jet mode of electrospray atomization have been published by Cloupeau & Prunet-Foch (1994) and Grace & Marijnissen (1994). Mestel (1994*a*) considered electrohydrodynamic flows through a conical meniscus at high Reynolds numbers and presented two models for a boundary layer at the meniscus surface. Shtern & Barrero (1994, 1995) constructed a model of a charged conical meniscus where the liquid velocity varies as $1/r$ (r is the distance from the cone apex) and studied swirling regimes. Melcher & Warren (1971) analysed a slender capillary jet pulled down under the electric field that was imposed by a cylindrical electrode concentrically surrounding the jet. Gañán-Calvo (1997*a,b*) discussed an extension of such a model to describe Taylor jets. Mestel (1994*b*, 1996) considered a cylindrical capillary jet carrying surface charge in a constant tangential

electric field and studied the jet stability for high and low Reynolds number flows. Thus, almost all available theoretical models are either based on some preliminary assumptions on the meniscus-jet shape and structure of electrohydrodynamic flow through the meniscus and emitted jet, or do not consider all regions (meniscus, jet and surrounding gas or vacuum) simultaneously. Although such approaches can often be justified by experimental investigations, they cannot derive the integral electrohydrodynamic picture of Taylor meniscus-jets from the basic principles of fluid mechanics and electrodynamics. The most interesting model giving such a picture (Fernández de la Mora 1992) describes the cone-jet mode with a negligible short jet that opens into the spray infinitesimally close to the cone apex. This model has successfully explained observed deflections of the cone angle from Taylor's value of 49.29° as an effect of the space charge of the spray. However, it was developed for the case of infinitely conductive liquids and, therefore, is not able to account for the scaling laws (1.1)–(1.2).

The most typical feature of the cone-jet mode of electrospray atomization is a sharp conical shape of the meniscus and the extreme thinness of the emitted jet. Its diameter is many orders of magnitude smaller than meniscus dimensions, while the jet length, i.e. the distance from the virtual cone apex to the point at which the jet opens into a spray of droplets, is usually comparable to or even greater than the meniscus dimensions. Such remarkable behaviour of the meniscus and jet suggests that an appropriate theoretical description might be obtained by singular perturbation methods directly from the basic equations of electrohydrodynamics. To do that, one must reveal perturbation quantities that would be small enough under conditions of electrospray experiments for which the cone-jet mode takes place.

Using the quantity r^* as the characteristic length in the transition region between the meniscus and jet, we can define the capillary (Ca), Weber (We), electrical Weber (We_E), and charge mobility (Mo) numbers for that region:

$$Ca \equiv \frac{\mu u^*}{\gamma}, \quad We \equiv \frac{\rho u^{*2} r^*}{\gamma}, \quad We_E \equiv \frac{\epsilon\epsilon_0 E^{*2} r^*}{\gamma}, \quad Mo \equiv \frac{k_i E^*}{u^*}. \tag{1.3a–d}$$

Here k_i is the electrical mobility of the ions which form the meniscus-jet charge, u^* and E^* are the effective scales of the liquid velocity and electric field strength in the transition region. They are determined by

$$u^* \equiv \frac{Q}{r^{*2}}, \quad E^* \equiv \frac{I}{K r^{*2}}. \tag{1.4a,b}$$

The non-dimensional numbers Ca, We, and We_E characterize the ratios of the viscous, inertial, and electrical forces, respectively, to the surface tension force in the transition region. Mo is the characteristic ratio in the transition region of the drift velocity of electric charge to the liquid velocity.

Substituting (1.4) into (1.3) and taking into account the expression (1.2b) for r^*, we can rewrite definitions (1.3) as

$$Ca = \frac{\eta^{2/3}}{\Pi}, \quad We = \eta^2, \quad We_E = \frac{f^2}{\epsilon}, \quad Mo = \frac{F}{\eta}, \tag{1.5a–d}$$

where Π, η, f, and F are independent non-dimensional parameters introduced by Fernández de la Mora & Loscertales (1994):

$$\Pi \equiv \left(\frac{\rho\epsilon\epsilon_0\gamma^2}{K\mu^3}\right)^{1/3}, \quad \eta \equiv \left(\frac{\rho K Q}{\epsilon\epsilon_0\gamma}\right)^{1/2}, \quad f \equiv \left(\frac{\epsilon I^2}{\gamma K Q}\right)^{1/2}, \quad F \equiv \frac{f k_i}{\epsilon}\left(\frac{\rho}{\epsilon_0}\right)^{1/2}. \tag{1.6}$$

The relations (1.5) fix the physical significance of Π, η, f, and F. It is worth noting that Π is an unique non-dimensional combination that depends only on the macroscopic properties of the liquid and not on the current or flow rate. The parameter f can also be interpreted as a non-dimensional current (Fernández de la Mora & Loscertales 1994) since its definition (1.6) can be rewritten in the form

$$f = I/I_s, \quad I_s \equiv r^* \sigma^* u^* = (\gamma K Q/\epsilon)^{1/2}, \quad \sigma^* \equiv (\epsilon_0 \gamma / r^*)^{1/2}, \tag{1.7a–c}$$

where σ^* and I_s are Taylor's characteristic values of the surface charge density and surface current in the transition region. Because of this, it will be more convenient to use f instead of We_E in the subsequent consideration.

Analysing the data published by Fernández de la Mora & Loscertales (1994), one can come to the conclusion that their parameters Π, η, f, F and dielectric constant ϵ fall into the ranges

$$0.07 \leqslant \Pi \leqslant 12, \quad 0.5 \leqslant \eta \leqslant 11, \quad 7 \leqslant f \leqslant 18, \quad 0.09 \leqslant F \leqslant 0.86, \quad 10 \leqslant \epsilon \leqslant 111 \tag{1.8}$$

for all the liquids that obey the scaling laws (1.1), (1.2). It is noteworthy that Π can be ~ 10 only for water solutions with $\epsilon \sim 10^2$, and f almost monotonically increases with an increase in ϵ (Fernández de la Mora & Loscertales 1994). The large number of governing parameters and their wide ranges do not allow an asymptotic analysis of the meniscus-jet structure, applicable in all cases, to be carried out. Thus, one has to consider various asymptotic regimes in the space of parameters (Ca, We, f, Mo, ϵ) or (Π, η, f, F, ϵ) and study corresponding meniscus-jet structures for all cases. The present paper deals with one such asymptotic regime for which

$$\delta \equiv We/f = \eta^2/f \ll 1, \tag{1.9}$$

while other parameters remain of the order of unity or may be much less (or greater) than unity if their magnitudes satisfy definite conditions (see § 4). This case corresponds to sufficiently low flow rates of the liquid since, taking into account (1.1) and (1.6), one can rewrite (1.9) as follows:

$$\delta = \text{const.} \times Q, \quad \text{const.} = \frac{\rho K}{\epsilon \epsilon_0 \gamma f_{exp}(\epsilon)}. \tag{1.10}$$

Here, const. is completely determined by the liquid properties and therefore does not change in experiments with the same liquid. For the smallest experimental values of Q which correspond to values of η near $\eta = 0.5$, the definition (1.9) yields $\delta \approx 10^{-2}$.

Section 2 of the paper introduces the non-dimensional variables and formulates the closed system of differential equations and boundary conditions that describe the problem in question. Section 3 derives simplified equations for the sufficiently thin jet. Section 4 offers a method of solving the system of governing equations in the regions of the meniscus, surrounding gas, and jet by means of asymptotic expansions in the small parameter δ. The basic solution and equations for the leading perturbation are derived. The solution to these equations is obtained and studied in § 5. The transition region is analysed in § 6, which also contains a derivation of the scaling laws (1.1), (1.2) from the theory developed. The physical meaning of the results obtained is discussed in § 7. It also summarizes the main conclusions. To examine the problem of the Taylor meniscus-jet structure, we use the techniques and terminology of fluid mechanics perturbation theory (Van Dyke 1975).

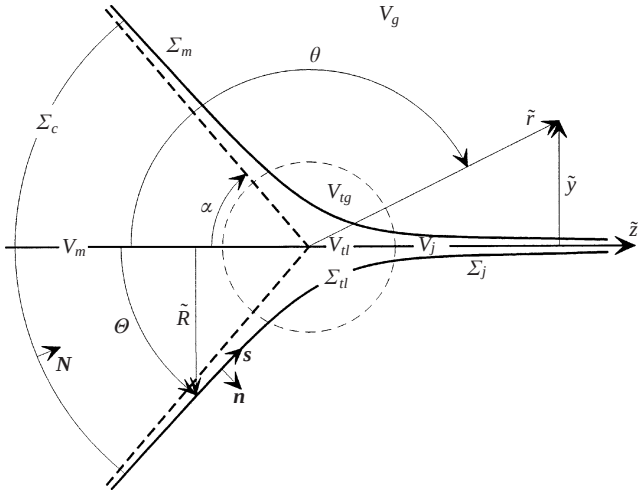

FIGURE 1. Sketch of coordinate systems and domains used for the meniscus-jet description. The solid lines show the liquid–gas interface $\Sigma_l = \Sigma_m \cup \Sigma_{tl} \cup \Sigma_j$ which is the union of the meniscus surface Σ_m, jet surface Σ_j, and liquid surface Σ_{tl} lying inside the transition region $V_t = V_{tl} \cup V_{tg}$. The dashed circle represents a boundary between the transition region V_t and the outer region $V = V_m \cup V_g \cup V_j$, which is the union of the meniscus, gas, and jet domains (V_m, V_g, and V_j, respectively). The dashed lines show the surface of Taylor's cone with no jet.

2. Formulation of the problem

Consider an axisymmetric non-swirling flow of an electrified liquid through a nearly conical semi-infinite meniscus whose apex emits a semi-infinite jet. It is convenient to use coordinate systems and regions sketched in figure 1, where $\tilde{r}, \theta, \chi$ and $\tilde{y}, \chi, \tilde{z}$ are spherical and cylindrical coordinates, respectively, Θ is the latitude of a point at the meniscus-jet surface, and $\tilde{R}$ is the distance from this point to the symmetry axis. Dimensional quantities are marked with tildes. The dashed lines show the conical surface Σ_T to which the meniscus surface asymptotically tends as $\tilde{z} \to -\infty$, and α is the semiangle of this cone. The dashed circle represents a relative boundary of the transition region $V_t = V_{tl} \cup V_{tg}$ that lies between the meniscus domain V_m and the jet domain V_j. Domains V_{tl} and V_{tg} consisting of the liquid and gas (or vacuum), respectively, are parts of V_t. The gas domain V_g is the region of surrounding gas (or vacuum) that is not included in the transition region V_t. The outer region $V = V_m \cup V_g \cup V_j$ lies outside the transition one. In figure 1, Σ_m and Σ_j are the meniscus–gas and jet–gas interfaces, respectively; Σ_l is the surface of the liquid domain $V_l = V_m \cup V_{tl} \cup V_j$; Σ_{tl} is a part of Σ_l lying inside the transition region V_t; Σ_c is a geometrical cross-section of the meniscus or jet; $\boldsymbol{n}$ and $\boldsymbol{N}$ are the unit vectors normal to Σ_l and Σ_c, respectively; $\boldsymbol{s}$ is the unit vector tangent to Σ_l along its generatrix, $\tilde{s}$ is the distance along it.

The current I and the liquid flow rate Q are defined as

$$I = 2\pi\tilde{R}(\tilde{\boldsymbol{j}}_s \cdot \boldsymbol{s}) + \int_{\Sigma_c(\tilde{R})} (\tilde{\boldsymbol{j}}_b \cdot \boldsymbol{N}) \mathrm{d}\Sigma_c, \quad Q = \int_{\Sigma_c} (\tilde{\boldsymbol{u}} \cdot \boldsymbol{N}) \mathrm{d}\Sigma_c, \tag{2.1a,b}$$

where $\tilde{\boldsymbol{j}}_s$ and $\tilde{\boldsymbol{j}}_b$ are the surface and bulk current densities, respectively, $\tilde{\boldsymbol{u}}$ is the liquid velocity, Σ_c is assumed to be a surface of revolution, and $\tilde{R}$ coincides with the radius of the circle $\Sigma_c \cap \Sigma_l$. Equalities (2.1*a,b*) are valid at any cross-section Σ_c due to charge and mass conservation laws; the liquid density ρ is considered to be constant. The

quantities $\tilde{\boldsymbol{j}}_s$ and $\tilde{\boldsymbol{j}}_b$ can be determined by the following relations:

$$\tilde{\boldsymbol{j}}_s = \tilde{\sigma}(\tilde{\boldsymbol{u}} + k_i(\tilde{\boldsymbol{E}} \cdot \boldsymbol{s})\boldsymbol{s}), \quad \tilde{\boldsymbol{j}}_b = K\tilde{\boldsymbol{E}} \quad (K = \text{const.}), \tag{2.2a,b}$$

where $\tilde{\sigma}$ is the surface charge density and $\tilde{\boldsymbol{E}}$ is the electric field strength. Thus, k_i is the electrical mobility of the surface ions. Validity of (2.2) was confirmed by Fernández de la Mora & Loscertales (1994) for all domains and all liquids that obey the scaling laws (1.1) and (1.2), except for the domain V_j in the case of the least conducting solutions of water and formamide.

2.1. *Non-dimensional variables*

In the case $Q = 0$ and $I = 0$, Taylor (1964) found an exact solution of the electrohydrostatic equations governing the equilibrium of an electrified meniscus. This solution can be written in our variables as follows:

$$\tilde{\phi} = 0 \quad \text{in} \quad V_m, \quad \tilde{\phi} = -\left(\frac{2\gamma\tilde{r}}{\epsilon_0 \tan\alpha}\right)^{1/2} \frac{Q_{1/2}(\cos\theta)}{Q'_{1/2}(\cos\alpha)} \quad \text{in} \quad V_g, \tag{2.3a,b}$$

$$\tilde{\sigma} = \left(\frac{2\epsilon_0\gamma}{\tilde{r}\tan\alpha}\right)^{1/2}, \quad \Theta = \alpha, \quad \tilde{R} = \tilde{r}\sin\alpha. \tag{2.4a–c}$$

Here $\tilde{\phi}$ is the dimensional electric field potential; $Q_{1/2}$ is the standard Legendre function of degree $1/2$ and order 0; $Q'_{1/2}$ is the derivative of $Q_{1/2}$ with respect to θ; and $\alpha = 0.27\pi = 49.29^\circ$ is the root of the equation $Q_{1/2}(\cos\alpha) = 0$. Relation (2.4*b*) determines the surface of the Taylor meniscus that turns out to be a cone of semiangle α with no jet. Thus, domains V_t and V_j are absent, and the electric field strength at semiaxis $\theta = \pi$ (or $\tilde{y} = 0$, $\tilde{z} > 0$) is given by

$$\tilde{E}(\tilde{r},\pi) = -\frac{\partial\tilde{\phi}}{\partial\tilde{r}} = C_T\left(\frac{\gamma}{\epsilon_0\tilde{z}}\right)^{1/2}, \quad C_T = \frac{1}{(2\tan\alpha)^{1/2}}\frac{Q_{1/2}(\cos\pi)}{Q'_{1/2}(\cos\alpha)} = 0.67. \tag{2.5a,b}$$

Taylor's solution (2.3*b*), (2.4*a*) and the non-dimensional current definition (1.7) suggest the following natural way to introduce non-dimensional variables r, y, z, R, s, ϕ, $\boldsymbol{E}$, $\boldsymbol{D}$, σ, $\boldsymbol{u}$, p, and p_g related to the dimensional ones marked with tildes:

$$r = \tilde{r}/L, \quad y = \tilde{y}/L, \quad z = \tilde{z}/L, \quad R = \tilde{R}/L, \quad s = \tilde{s}/L, \quad \phi = \tilde{\phi}/\phi^\circ, \tag{2.6}$$

$$\boldsymbol{E} = \tilde{\boldsymbol{E}}/E^\circ, \quad \sigma = \tilde{\sigma}/\sigma^\circ, \quad \boldsymbol{D} = \tilde{\boldsymbol{D}}/\sigma^\circ, \quad \boldsymbol{u} = \tilde{\boldsymbol{u}}/u^\circ, \quad p = \tilde{p}/p^\circ, \quad p_g = \tilde{p_g}/p^\circ, \tag{2.7}$$

$$\phi^\circ \equiv \left(\frac{\gamma L}{\epsilon_0}\right)^{1/2}, \quad E^\circ \equiv \frac{\phi^\circ}{L}, \quad \sigma^\circ \equiv \epsilon_0 E^\circ, \quad u^\circ \equiv \frac{I_s}{L\sigma^\circ} = \left(\frac{KQ}{\epsilon\epsilon_0 L}\right)^{1/2}, \quad p^\circ \equiv \frac{\gamma}{L}, \tag{2.8}$$

where $\boldsymbol{D}$ is the electric displacement; p and p_g are the pressure of the liquid and surrounding gas, respectively; I_s is determined by (1.7*b*); L is the primary reference length in the outer region $V = V_m \cup V_g \cup V_j$; and the characteristic values of the other quantities in the outer region are marked with circles.

Obviously, we cannot simply define $L = r^*$ because the meniscus dimensions and jet length are much larger than r^*. The length L should be found while one is solving the problem in question since neither this problem itself nor Taylor's solution contains any geometrical scale for the outer region. It is convenient and always possible to choose the quantity L so that inertial, capillary, and electrical effects in the jet would be finite at $\tilde{z} \sim L$ as $\delta \to 0$. In § 3, we shall see that such a condition is fulfilled if we

put

$$L \equiv \delta^{-2/3} r^*. \tag{2.9}$$

2.2. *Basic equations and boundary conditions*

In formulating basic equations we shall use relations (2.2*a,b*) and the following additional hypotheses:

(i) the liquid flow and electric field are steady state;
(ii) the surrounding gas is at rest and, therefore, its pressure p_g is constant;
(iii) the liquid charge is concentrated at the meniscus-jet surface.

The first assumption corresponds to numerous observations of the cone-jet mode of electrospray atomization, although it excludes unsteady-state processes and stability problems from further consideration. The next one is justified by the ratio μ_g/μ being small enough, where μ_g is the viscosity coefficient of the surrounding gas. In conclusion, the third hypothesis is correct under the condition

$$\left(\frac{r_D}{\tilde{R}}\right)^2 \ll 1 \qquad \left(r_D^2 = \frac{\epsilon\,\epsilon_0 \kappa T}{(e_+^2 n_+ + e_-^2 n_-) N_A}\right), \tag{2.10}$$

where r_D is the thickness of Debye's surface boundary layer in which the charge is actually distributed; $n_\pm$ are the molar concentrations of ions in the liquid; $e_\pm$ are the charges of ions; T is the liquid temperature; κ is Boltzmann's constant; N_A is Avogadro's number. The inequality (2.10) appears to be always fulfilled in electrospray atomization. For example, by using the data published by Fernández de la Mora & Loscertales (1994) one can verify that $r_D/R^* \leqslant 0.1$ for all liquids which were used in their work to obtain scaling laws (1.1), (1.2).

The liquid flow through the meniscus, transition region, and jet as well as the electric field distribution inside and outside the above regions are governed by the electrohydrodynamics equations that can be written in non-dimensional variables (2.6), (2.7) as follows:

$$\nabla \cdot \boldsymbol{D} = 0, \quad \boldsymbol{E} = -\nabla \phi \quad \text{in} \quad V_k \quad (k = l, g, tg), \tag{2.11a,b}$$

$$\boldsymbol{D} = \epsilon \boldsymbol{E} \quad \text{in} \quad V_l; \quad \boldsymbol{D} = \boldsymbol{E} \quad \text{in} \quad V_k \quad (k = g, tg), \tag{2.12a,b}$$

$$\nabla \cdot \boldsymbol{u} = 0, \quad \delta f(\boldsymbol{u} \cdot \nabla)\boldsymbol{u} = -\nabla p + \delta^{1/3} Ca \nabla^2 \boldsymbol{u} \quad \text{in} \quad V_l. \tag{2.13a,b}$$

This system should be supplemented with non-dimensional boundary conditions at Σ_l:

$$[\phi]_l^g = 0, \quad \sigma = [\boldsymbol{n} \cdot \boldsymbol{D}]_l^g, \quad \delta \frac{\mathrm{d}}{\mathrm{d}s}\left(R\sigma\left(u + \frac{Mo}{f}(\boldsymbol{s} \cdot \boldsymbol{D})\right)\right) = R(\boldsymbol{n} \cdot \boldsymbol{D}_l), \tag{2.14a–c}$$

$$\boldsymbol{n} \cdot \boldsymbol{u} = 0, \quad \delta^{1/3} Ca\left(\boldsymbol{s} \cdot \frac{\mathrm{d}\boldsymbol{u}}{\mathrm{d}n} + \boldsymbol{n} \cdot \frac{\mathrm{d}\boldsymbol{u}}{\mathrm{d}s}\right) = \frac{\sigma}{\epsilon}(\boldsymbol{s} \cdot \boldsymbol{D}_l) + \frac{\mathrm{d}\Gamma}{\mathrm{d}s}, \tag{2.15a,b}$$

$$p - p_g - 2\delta^{1/3} Ca\, \boldsymbol{n} \cdot \frac{\mathrm{d}\boldsymbol{u}}{\mathrm{d}n} = -\left[(\boldsymbol{n} \cdot \boldsymbol{E})(\boldsymbol{n} \cdot \boldsymbol{D}) - \tfrac{1}{2}\boldsymbol{E} \cdot \boldsymbol{D}\right]_l^g + H\Gamma, \tag{2.16}$$

where

$$\Gamma \equiv \frac{\gamma_s}{\gamma}, \quad H = \frac{2}{(r^2 \sin^2 \Theta)'}\left(\frac{r \sin \Theta (r \cos \Theta)'}{(1 + r^2 \Theta'^2)^{1/2}}\right)', \quad R = r \sin \Theta(r). \tag{2.17a–c}$$

We also use the notations: $[a]_l^g \equiv a_g - a_l$; a_l and a_g are the values of any quantity a at Σ_l inside and outside V_l, respectively; H is the normal curvature of the meniscus-jet surface Σ_l; $\theta = \Theta(r)$ is the equation for Σ_l in the spherical coordinates; γ_s is the coefficient of meniscus-jet surface tension. Primes denote derivatives with respect to r. If Σ_l is the surface of Taylor's cone (2.4b), relation (2.17b) yields the following expression for its mean normal curvature:

$$H = \frac{1}{r \tan \alpha} \quad \text{at} \quad \Sigma_T. \tag{2.18}$$

Boundary conditions (2.14a,c) express electric potential continuity and charge conservation at the interface Σ_l. Equation (2.14b) yields the surface charge density in terms of the electric field jump at Σ_l. Equality (2.15a) means that the surface Σ_l consists of liquid streamlines. Conditions (2.15b) and (2.16) express, respectively, the balance of shear and normal stresses of the liquid, surrounding gas and electric field at the interface Σ_l. While formulating the boundary conditions, we have used an expression for the normal curvature of the surface of revolution (Dubrovin, Fomenko & Novikov 1984). The last term in equation (2.15b) takes into account the surface stresses in the case where the surface tension does not remain constant (Scriven 1960). This term is usually negligible at the meniscus surface Σ_m since the value of γ_s is almost equal to $\gamma = \text{const.}$ at Σ_m. However, γ_s might be sufficiently larger than γ at the surfaces Σ_{tl} and Σ_j of the transition liquid domain and jet due to the smallness of their diametrical dimensions and very high level of the ion concentration in these regions. The investigation of the liquid surface tension under such extreme conditions is an independent problem that is not the goal of this paper. We assume that the ratio $\Gamma = \gamma_s/\gamma$ is the given constant for the jet and it is equal to unity for the meniscus:

$$\Gamma = 1 \quad \text{at} \quad \Sigma_m, \quad \Gamma = \text{const.} \quad \text{at} \quad \Sigma_j. \tag{2.19a,b}$$

Evidently, all results obtained below will also be valid in the case $\gamma_s \equiv \gamma$, if we put $\Gamma \equiv 1$.

In conclusion, conditions (2.1) are rewritten in the non-dimensional form as follows:

$$2\pi\delta R\sigma \left(u + \frac{Mo}{f}(\boldsymbol{s} \cdot \boldsymbol{D}) \right) = \delta f - \int_{\Sigma_c(R)} (\boldsymbol{D} \cdot \boldsymbol{N}) \mathrm{d}\Sigma_c, \quad \int_{\Sigma_c} (\boldsymbol{u} \cdot \boldsymbol{N}) \mathrm{d}\Sigma_c = \delta. \tag{2.20a,b}$$

Consideration of the problem in the infinite domains V_m, V_g and V_j requires some conditions at $r \to \infty$ to be imposed. The simplest form of such conditions seems to arise from the assumption that the unknown solution of equations (2.11)–(2.16) (for $Q \neq 0$ and $I \neq 0$) tends asymptotically to Taylor's solution as $r \to \infty$. In this case, the radius and charge of the jet should vanish as $z \to \infty$. Accordingly, one can write down

$$\phi \to 0, \quad \boldsymbol{u} \to 0 \quad \text{as} \quad r \to \infty \quad \text{in} \quad V_m, \tag{2.21a,b}$$

$$(\sigma - \sigma_T)/\sigma_T \to 0, \quad \Theta \to \alpha \quad \text{as } r \to \infty \quad \text{at} \quad \Sigma_m, \tag{2.22a,b}$$

$$(\phi - \phi_T)/\phi_T \to 0 \quad \text{as } r \to \infty \quad \text{in} \quad V_g \cup V_j, \tag{2.23}$$

$$R\sigma \to 0, \quad R \to 0 \quad \text{as } r \to \infty \quad \text{in} \quad V_j, \tag{2.24a,b}$$

where quantities ϕ_T, σ_T, and R_T are a non-dimensional form of Taylor's functions (2.3*b*) and (2.4*a,c*):

$$\phi_T = -2C_T r^{1/2}\frac{Q_{1/2}(\cos\theta)}{Q_{1/2}(\cos\pi)}, \quad \sigma_T = \left(\frac{2}{r\tan\alpha}\right)^{1/2}, \quad R_T = r\sin\alpha, \tag{2.25a–c}$$

and C_T is the constant defined by (2.5*b*).

3. Governing equations for the thin jet

The theory of slender liquid jets is a discipline with a long history and a wide variety of applications (Anno 1977). A nonlinear analysis of the breakup of uncharged capillary jets has recently been performed by Eggers & Dupont (1994), Eggers (1995), Papageorgiou (1995*a, b*). They derived a set of one-dimensional governing equations for the jet directly from the Navier–Stokes equations.

It is more convenient, however, to use the integrated form of energy equation in asymptotic analysis of charged jets:

$$\left[\int_{\Sigma_2} - \int_{\Sigma_1}\right]\left\{\left(\tfrac{1}{2}\delta f u^2 + p\right)(\boldsymbol{u}\cdot\boldsymbol{N}) - 2\delta^{1/3}Ca(\boldsymbol{u}\cdot\boldsymbol{e}\cdot\boldsymbol{N})\right\}\mathrm{d}\Sigma_c$$
$$= \int_{\Sigma_{12}}\frac{\sigma}{\epsilon}(\boldsymbol{s}\cdot\boldsymbol{D}_l)u\mathrm{d}\Sigma_j - 2\delta^{1/3}Ca\int_{V_{12}}(\boldsymbol{e}\cdot\boldsymbol{e})\mathrm{d}V_j, \tag{3.1}$$

where

$$(\boldsymbol{u}\cdot\boldsymbol{e}\cdot\boldsymbol{N}) = u^a e_{ab}N^b, \quad (\boldsymbol{e}\cdot\boldsymbol{e}) = e_{ab}e^{ab}, \quad e_{ab} = \tfrac{1}{2}(\nabla_a u_b + \nabla_b u_a), \tag{3.2a–c}$$

u_a, N^b, e_{ab} are components of the vectors $\boldsymbol{u}$, $\boldsymbol{N}$ and second-order strain rate tensor $\boldsymbol{e}$, respectively; ∇_a is the covariant derivative ($a, b = 1, 2, 3$); Σ_2 and Σ_1 are any two positions of the cross-section Σ_c within the domain V_j, Σ_2 being to the right of Σ_1 (see figure 1); Σ_{12} and V_{12} are parts of Σ_j and V_j, that lie between the cross-sections Σ_1 and Σ_2. To obtain equation (3.1) one should multiply relation (2.13*b*) scalarly by $\boldsymbol{u}$ and then integrate it over the volume V_{12} using Gauss' theorem and taking into account continuity equation (2.13*a*) and conditions (2.15*a,b*), (2.19*b*).

3.1. *Infinitesimally thin jet*

We shall study the liquid flow through the jet in the asymptotic limit $R \to 0$. In this case the domain V_j becomes one-dimensional and the partial differential equations that govern the liquid flow can be reduced to ordinary ones. To do that one should expand the unknown solution to those equations into power series in the radial coordinate y (Eggers & Dupont 1994). Thus, we shall use the following expressions for $\boldsymbol{u}$, p, and ϕ in the domain V_j:

$$u_z = u_0(z) + \tfrac{1}{2}y^2u_2(z) + O(y^4), \tag{3.3a}$$

$$u_y = -\tfrac{1}{2}yu_0'(z) + O(y^3) \quad \left(u_0'(z) = \mathrm{d}u_0/\mathrm{d}z\right), \tag{3.3b}$$

$$p = p_0(z) + \tfrac{1}{2}y^2p_2(z) + O(y^4), \tag{3.3c}$$

$$\phi = \phi_0(z) + \tfrac{1}{2}y^2\phi_2(z) + O(y^4), \tag{3.3d}$$

where u_y and u_z are, respectively, the radial and axial components of the liquid velocity in cylindrical coordinates y, χ, z, and relation (3.3*b*) follows from (2.13*a*) and

(3.3*a*). In this case, equations (3.2*b*,*c*) yield

$$e_{yy} = e_{\chi\chi} = -\frac{e_{zz}}{2} = -\frac{u_0'}{2} + O(y^2), \quad e_{yz} = \frac{y}{2}\left(u_2 - \frac{u_0''}{2}\right) + O(y^3), \tag{3.4}$$

$$e_{y\chi} = e_{\chi z} = 0, \quad (\mathbf{e}\cdot\mathbf{e}) = e_{yy}^2 + e_{\chi\chi}^2 + e_{zz}^2 + 2e_{yz}^2 = \tfrac{3}{2}u_0'^2 + O(y^2), \tag{3.5}$$

where e_{yy}, $e_{\chi\chi}$, e_{zz}, e_{yz}, $e_{y\chi}$, and $e_{\chi z}$ are the physical components of tensor $\mathbf{e}$ in cylindrical coordinates y, χ, z.

Eliminating the term H from equation (2.16) by means of (2.17*b*) and then substituting expansions (3.3) into (2.16), (3.1), and (2.20) we derive the following relations for leading terms u_0, p_0, ϕ_0 in the jet in the limit $R \to 0$:

$$p_0 - p_g + \delta^{1/3} Ca\, u_0' = -\tfrac{1}{2}(\sigma^2 + (\epsilon - 1)\phi_0'^2) + \frac{\Gamma}{R}, \tag{3.6}$$

$$\left[\left(\tfrac{1}{2}\delta f u_0^2 + p_0 - 2\delta^{1/3} Ca\, u_0'\right) R^2 u_0\right]_{z_1}^{z_2} = \int_{z_1}^{z_2} \left(-2\sigma\phi_0' R u_0 - 3\delta^{1/3} Ca R^2 u_0'^2\right) \mathrm{d}z, \tag{3.7}$$

$$2\pi\delta R\sigma\left(u_0 - \frac{\epsilon Mo}{f}\phi_0'\right) = \delta f + \pi\epsilon R^2\phi_0', \quad \pi R^2 u_0 = \delta, \tag{3.8a,b}$$

where primes denote derivatives with respect to z. We have also used expressions (2.11*b*), (2.12) for quantities $\boldsymbol{E}$, $\boldsymbol{D}$ (in equations (2.16), (3.1), and (2.20*a*)), eliminated $(\boldsymbol{D}_g \cdot \boldsymbol{n})$ by means of (2.14*b*) and taken into account relations (2.14*a*), and (3.5).

Replacing integral equation (3.7) with differential one at $z_1 \to z_2$ and then eliminating quantities p_0 and R from it by means of equations (3.6) and (3.8*b*), we obtain (after some algebraic transformations) the final equations to describe the jet in the asymptotic limit $R \to 0$:

$$\left(\tfrac{1}{2}(\delta u_0)^2 + \frac{\Gamma}{f}(\pi\delta u_0)^{1/2} - \frac{\delta}{2f}\left(\sigma^2 + (\epsilon - 1)\phi_0'^2\right)\right)' = -\frac{q u_0}{f}\phi_0' + \frac{3\delta^{1/3} Ca}{f}(\delta u_0)\left(\frac{u_0'}{u_0}\right)', \tag{3.9}$$

$$\frac{q u_0}{f}\left(1 - \frac{\epsilon Mo}{f u_0}\phi_0'\right) = 1 + \frac{\epsilon}{f u_0}\phi_0', \quad \pi R^2 u_0 = \delta, \quad q \equiv 2\pi R\sigma, \tag{3.10a–c}$$

where q is the charge per unit length of the jet. To derive (3.10*a*), we have also eliminated the jet radius R from the right-hand side of (3.8*a*) by means of (3.8*b*). Equations (3.6), (3.9), (3.10) form a closed system for the unknowns p_0, u_0, σ, R, q, if $\phi_0(z)$ is given. At $\sigma = q = \phi_0 \equiv 0$ relations (3.6), (3.9), (3.10*b*) are equivalent to those obtained by Eggers & Dupont (1994). It is noteworthy that relations (3.6) and (3.10) are simple algebraic equations to express quantities p_0, σ, R, q, in terms of $u_0(z)$ and $\phi_0(z)$. Therefore, only equation (3.9) for $u_0(z)$ has to be solved. We shall see that it is simplified greatly in the limit $\delta \to 0$.

The functions $\phi_0(z)$ and $q(z)$ must obey the conditions of asymptotic matching with the electric potential $\phi(r, \theta)$ outside the jet:

$$\phi(r, \theta) \to \phi_0(z), \quad 2\pi \sin\theta \frac{\partial\phi}{\partial\theta} \to q(z) \quad \text{as} \quad r = z, \quad \pi - \theta = \frac{R}{z} \to 0. \tag{3.11a,b}$$

These relations follow from boundary conditions (2.14*a*,*b*) and expansion (3.3*d*).

3.2. *Small Weber numbers*

We shall study the asymptotic limit $\delta \equiv We/f \to 0$ which may correspond to sufficiently small values of the Weber number $We \equiv \eta^2$. For the smallest values of η from the range (1.8), the meniscus shape observed in experiments almost coincides with the cone of Taylor's semiangle α (Fernández de la Mora 1992). Given that fact, we shall seek such asymptotic solutions of equations (2.11)–(2.16) for which the basic solution, i.e. zeroth approximation, is Taylor's one. Equations (2.14) and (2.20) suggest that the leading perturbations of the electric field in the liquid meniscus and surrounding gas are of the order of δ as $\delta \to 0$. In this case, condition (3.11*b*) yields $q \sim \delta$ since Taylor's solution is regular as $\theta \to \pi$. As a result, we obtain from (2.15*b*) and (3.10):

$$u \sim \frac{\delta^{2/3}}{\epsilon Ca} \quad \text{at} \quad r \sim 1 \quad \text{in} \quad V_m; \quad u_0 \sim \frac{1}{\delta}, \quad R \sim \delta \quad \text{at} \quad z \sim 1 \quad \text{in} \quad V_j. \quad (3.12a,b)$$

Thus, the first (inertial) and second (capillary) terms on the left-hand side of (3.9) and the first (electrical) term on the right-hand side of (3.9) remain finite as $\delta \to 0$.

It is noteworthy that the reciprocal of the quantity $\delta^{1/3}Ca/f$, that appears in (3.9), can be interpreted as the Reynolds longitudinal number of the jet which is constructed as follows:

$$Re_{\|} \equiv \frac{\rho \tilde{u}_j L}{\mu} = \frac{f}{\delta^{1/3} Ca}, \quad \tilde{u}_j \equiv \frac{u^\circ}{\delta}, \tag{3.13}$$

where the dimensional quantities L and u° are defined by relations (2.9) and (2.8). Taking into account estimation (3.12*a*), we can also find the Reynolds number for the meniscus at $r \equiv \tilde{r}/L \sim 1$:

$$Re_m \equiv \frac{\rho \tilde{u}_m L}{\mu} = \frac{\delta^{4/3} f}{\epsilon Ca^2}, \quad \tilde{u}_m \equiv \frac{\delta^{2/3}}{\epsilon Ca} u^\circ. \tag{3.14}$$

Since

$$Re_{\|} \to \infty, \quad Re_m \to 0 \quad \text{as} \quad \delta \to 0 \quad \text{and} \quad Ca, f, \epsilon = \text{const.}, \tag{3.15}$$

we can expect that the last (viscous) term in (3.9) and the first (inertial) term in (2.13*b*) for the meniscus are negligible.

4. Outer asymptotic expansions and equations

Let us seek an asymptotic solution of equations (2.11)–(2.16) in the domains V_m and V_g in the form

$$\left.\begin{aligned} &\boldsymbol{D} = \boldsymbol{D}_{m0} + \delta \boldsymbol{D}_{m1} + o(\delta^{4/3}), \quad \boldsymbol{E} = \boldsymbol{E}_{m0} + \delta \boldsymbol{E}_{m1} + o(\delta^{4/3}) \\ &\phi = \phi_{m0} + \delta \phi_{m1} + o(\delta^{4/3}), \quad \boldsymbol{u} = \boldsymbol{U}_0 + \frac{\delta^{2/3}}{\epsilon\, Ca} \boldsymbol{U}_1 + \delta \boldsymbol{U}_2 + o(\delta) \\ &p = P_0 + \frac{\delta}{\epsilon} P_1 + \delta^{4/3} Ca\, P_2 + o(\delta^{4/3}) \end{aligned}\right\} \text{ in } V_m, \tag{4.1}$$

$$\Theta(r) = \Theta_0 + \delta \Theta_1 + o(\delta), \quad \sigma(r) = \sigma_0 + \delta \sigma_1 + o(\delta) \quad \text{at} \quad \Sigma_m, \tag{4.2}$$

$$\phi = \phi_{g0} + \delta \phi_{g1} + o(\delta), \quad \boldsymbol{D} = \boldsymbol{E} = \boldsymbol{E}_{g0} + \delta \boldsymbol{E}_{g1} + o(\delta) \quad \text{in} \quad V_g. \tag{4.3}$$

It should be recalled here that we use the spherical coordinates r, χ to mark points at the meniscus surface Σ_m as we write down its equation in the form $\theta = \Theta(r)$. Thus, the perturbations of the meniscus latitude Θ and surface charge density σ are

calculated at $r = \text{const.}$ in (4.2). If the unperturbed meniscus coincides with Taylor's cone, i.e. $\Theta_0 = \alpha$, the product $r\Theta_1$ will represent the (scaled) normal displacement of the meniscus surface Σ_T as $\delta \to 0$ and $r = \text{const.}$

We shall also seek an asymptotic solution of equations (3.6), (3.9)–(3.11) at the semiaxis $\theta = \pi$ which replaces the domain V_j in the limit $R \to 0$ in the form

$$\left.\begin{aligned} &u_0 = \frac{1}{\delta}(U_j + o(1)), \quad p_0 = \frac{1}{\delta}(P_j + o(1)) \\ &R = \delta(R_j + o(1)), \quad \sigma = \sigma_j + o(1) \\ &q = \delta(q_j + o(1)), \quad \phi_0 = \phi_{g0} + \Delta_\phi(\delta)\Phi + o(\Delta_\phi) \end{aligned}\right\} \text{ at } \theta = \pi. \tag{4.4}$$

Here, $\Delta_\phi(\delta)$ is the gauge function that tends to zero as $\delta \to 0$ and is determined in the course of solving the problem. Since it is described by parameters Ca, f, Mo, ϵ, and Γ besides δ, one must specify their limiting behaviour as $\delta \to 0$. We assume that the quantities

$$\frac{1}{Re_\parallel} \equiv \frac{\delta^{1/3} Ca}{f}, \quad \Delta \equiv \frac{\delta^{2/3}}{\epsilon\, Ca}, \tag{4.5a,b}$$

which appear in relations (3.9) and (3.12a), respectively, also tend to zero:

$$Re_\parallel^{-1} = o(1), \quad \Delta = o(1) \quad \text{as} \quad \delta \to 0, \tag{4.6a,b}$$

while f, Mo, ϵ, and Γ remain bounded. According to (3.12a) and (4.1), relation (4.6b) means that the velocity perturbation vanishes in the meniscus at small δ as it should since the electric field distribution tends to Taylor's equilibrium distribution as $\delta \to 0$.

Obviously, conditions (4.6) are fulfilled if $Ca = \text{const.}$ as $\delta \to 0$. But this restriction is not necessary. They may also be valid if Ca tends to zero or infinity at appropriate relative rates. For example, conditions (4.6) are fulfilled if Ca scales as $\delta^{1/3}$. This case corresponds to $\Pi = \text{const.}$ as $\delta \to 0$ since (1.5) and (1.9) yield $Ca = \delta^{1/3} f^{1/3} \Pi^{-1}$, where the non-dimensional parameter Π depends only on the liquid properties (see (1.6)). Taking into account (1.5a) and (1.8), one can readily verify that $Re_\parallel^{-1} \ll 1$, $\Delta \ll 1$, $\delta \ll 1$ for all values of Π, f, ϵ from ranges (1.8) if η is near its smallest value from (1.8).

It should be emphasized that the leading perturbation of the jet parameters u_0, p_0, σ does not vanish as $\delta \to 0$ (see (4.4)). The same is true for the perturbation of $\boldsymbol{E} \cdot \boldsymbol{n}$ at the jet surface Σ_j, although the perturbation of ϕ at Σ_j vanishes. Yet, the region in which those non-vanishing perturbations are concentrated does vanish as $\delta \to 0$ since the radius and charge of the jet tend to zero according to expansions (4.4). Such behaviour is a typical feature of singular perturbation problems (Van Dyke 1975).

4.1. *Equations for the leading perturbation in $V_m \cup V_g$*

Let us substitute expansions (4.1)–(4.3) into equations (2.11)–(2.16), (2.20), (2.21)–(2.23) and take into account relations (2.17b,c), (2.19a) and conditions (4.6). As a result, first of all, we find the basic solution (zeroth approximation in δ) to coincide with Taylor's one:

$$\phi_{m0} = \boldsymbol{E}_{m0} = \boldsymbol{D}_{m0} = 0, \quad \boldsymbol{U}_0 = 0, \quad P_0 = p_g \quad \text{in} \quad V_m; \tag{4.7a–c}$$

$$\sigma_0 = \sigma_T, \quad \Theta_0 = \alpha \quad \text{at} \quad \Sigma_m; \tag{4.8a,b}$$

$$\phi_{g0} = \phi_T, \quad \boldsymbol{D}_{g0} = \boldsymbol{E}_{g0} = -\nabla\phi_T \quad \text{in} \quad V_g. \tag{4.9a,b}$$

Then we obtain that the (scaled) leading perturbation (first approximation in δ) must satisfy a system of simplified relations. It includes the governing equations in the meniscus and gas domains:

$$\nabla \cdot \boldsymbol{D}_{m1} = 0, \quad \boldsymbol{E}_{m1} = -\nabla \phi_{m1}, \quad \boldsymbol{D}_{m1} = \epsilon \boldsymbol{E}_{m1} \quad \text{in} \quad V_m, \tag{4.10a–c}$$

$$\nabla \cdot \boldsymbol{U}_k = 0, \quad 0 = -\nabla P_k + \nabla^2 \boldsymbol{U}_k \quad \text{in} \quad V_m \quad (k = 1, 2), \tag{4.11a,b}$$

$$\nabla \cdot \boldsymbol{E}_{g1} = 0, \quad \boldsymbol{E}_{g1} = -\nabla \phi_{g1} \quad \text{in} \quad V_g; \tag{4.12a,b}$$

the boundary conditions at the meniscus surface:

$$\phi_{g1} - r\sigma_T \Theta_1 = \phi_{m1}, \quad \sigma_1 = \boldsymbol{n} \cdot \boldsymbol{E}_{g1} - \frac{\sigma_T \Theta_1}{\tan \alpha}, \quad 0 = \boldsymbol{n} \cdot \boldsymbol{D}_{m1} \ \text{at} \ \Sigma_T, \tag{4.13a–c}$$

$$\boldsymbol{n} \cdot \boldsymbol{U}_1 = 0, \quad \boldsymbol{s} \cdot \frac{\mathrm{d}\boldsymbol{U}_1}{\mathrm{d}n} = \sigma_T (\boldsymbol{s} \cdot \boldsymbol{D}_{m1}), \quad \boldsymbol{n} \cdot \boldsymbol{U}_2 = 0, \quad \boldsymbol{s} \cdot \frac{\mathrm{d}\boldsymbol{U}_2}{\mathrm{d}n} = 0 \ \text{at} \ \Sigma_T, \tag{4.14a–d}$$

$$\frac{1}{\epsilon}\left(P_1 - 2\boldsymbol{n} \cdot \frac{\mathrm{d}\boldsymbol{U}_1}{\mathrm{d}n}\right) = -\sigma_T (\boldsymbol{n} \cdot \boldsymbol{E}_{g1}) + \frac{\Theta_1}{r \tan^2 \alpha} - \frac{1}{r}(r(r\Theta_1)')' \quad \text{at} \quad \Sigma_T; \tag{4.15}$$

the integral conditions at the cross-section Σ_c:

$$\int_{\Sigma_c} (\boldsymbol{D}_{m1} \cdot \boldsymbol{N}) \mathrm{d}\Sigma_c = f, \quad \int_{\Sigma_c} (\boldsymbol{U}_1 \cdot \boldsymbol{N}) \mathrm{d}\Sigma_c = 0, \quad \int_{\Sigma_c} (\boldsymbol{U}_2 \cdot \boldsymbol{N}) \mathrm{d}\Sigma_c = 1; \tag{4.16a–c}$$

and the limiting conditions at infinity:

$$\phi_{m1} \to 0, \quad \boldsymbol{U}_1 \to 0, \quad \boldsymbol{U}_2 \to 0 \quad \text{as} \quad r \to \infty \quad \text{in} \quad V_m, \tag{4.17a–c}$$

$$\sigma_1/\sigma_T \to 0, \quad \Theta_1 \to 0 \quad \text{as} \quad r \to \infty \quad \text{at} \quad \Sigma_T, \tag{4.18a,b}$$

$$\phi_{g1}/\phi_T \to 0 \quad \text{as} \quad r \to \infty \quad \text{in} \quad V_g. \tag{4.19}$$

It should be observed that conditions (4.13)–(4.15) are already formulated at the unperturbed surface of Taylor's cone Σ_T.

While deriving the boundary conditions for the leading perturbation, we have taken into account Taylor's field shift due to the perturbation of the meniscus surface Σ_m:

$$\phi_T\Big|_{\theta=\Theta(r)} = \phi_T\Big|_{\theta=\alpha} + \delta\Theta_1 \frac{\partial \phi_T}{\partial \theta}\Big|_{\theta=\alpha} = -\delta r \sigma_T \Theta_1, \tag{4.20a}$$

$$\left(\boldsymbol{n} \cdot \boldsymbol{E}_T\right)_{\theta=\Theta(r)} = \left(\boldsymbol{n} \cdot \boldsymbol{E}_T\right)_{\theta=\alpha} + \delta\Theta_1 \left(\boldsymbol{n} \cdot \frac{\partial \boldsymbol{E}_T}{\partial \theta}\right)_{\theta=\alpha} = \sigma_T - \frac{\delta \sigma_T \Theta_1}{\tan \alpha}. \tag{4.20b}$$

These expressions follow directly from general properties of Taylor's field:

$$\boldsymbol{E}_T = -\nabla \phi_T, \quad \nabla \cdot \boldsymbol{E}_T = 0 \quad \text{in} \quad V_g; \quad \phi_T = 0, \quad \sigma_T = \boldsymbol{n} \cdot \boldsymbol{E}_T \quad \text{at} \quad \Sigma_T; \tag{4.21}$$

with allowance for the fact that $\delta r \Theta_1$ is the meniscus surface perturbation along the normal $\boldsymbol{n}$. As a result, the additional terms proportional to Θ_1 have appeared in (4.13*a,b*) and (4.15).

4.2. *Equations for the leading perturbation in V_j*

Now let us substitute expansions (4.4) into equations (3.6), (3.9)–(3.11), and (2.24), make use of relations (2.19*b*) and (4.6), and take into account the expression for Taylor's field at the semiaxis $z > 0$ (i.e. at $\theta = \pi$):

$$-\phi'_{g0} = -\phi'_T = C_T z^{-1/2} \qquad (C_T = 0.67) \tag{4.22}$$

that follows from (4.9*a*), (2.25*a*), and (2.5*b*). As a result, we find that the functions U_j, P_j, R_j, σ_j, q_j, Φ must obey the governing equations at $z > 0$:

$$\left(\frac{1}{2}U_j^2 + \frac{\Gamma}{f}(\pi U_j)^{1/2}\right)' = C_T z^{-1/2}, \tag{4.23}$$

$$P_j = \frac{\Gamma}{R_j}, \quad q_j U_j = f, \quad \pi R_j^2 U_j = 1, \quad q_j = 2\pi R_j \sigma_j; \tag{4.23a–d}$$

the conditions of matching with the gas domain solution:

$$\delta\phi_{g1}(r,\theta) \to \Delta_\phi \Phi(z), \ 2\pi \sin\theta \frac{\partial \phi_{g1}}{\partial \theta} \to q_j(z) \ \text{ as } \ r = z, \ \pi - \theta = \frac{\delta R_j}{z} \to 0; \tag{4.24a,b}$$

and the conditions at infinity:

$$q_j \to 0, \quad R_j \to 0 \quad \text{as} \quad z \to \infty. \tag{4.25a,b}$$

All functions in equations (4.23), (4.24) are defined at the semiaxis $z > 0$ which replaces the jet domain V_j in the limit $\delta \to 0$, and primes denote derivatives with respect to z. Equation (4.23) takes into account the liquid inertia (the term with U_j^2), surface tension (the term with Γ), and electrical force (the term $C_T z^{-1/2}$).

Relation (4.24*b*) means that the jet is free from charge relaxation effects. It should be emphasized that the original equations ((2.2) for the surface and bulk currents and (2.14*c*), (2.20*a*) for the surface charge) take into account the bulk conductivity and the surface ion mobility. They remain in the general equation (3.10*a*) for the jet charge. However, the perturbation theory yields that this equation will be free from charge relaxation effects in the first approximation in δ. Such behaviour is due to the fact that the radius and velocity of the jet tend to zero and infinity, respectively, as $\delta \to 0$ while its surface charge density and electric field remain finite. As a result, the current of ions from the electric field vanishes in the jet, and all of its current is carried by the flow of liquid.

It is also worth noting that (3.3*a*,*d*) and (3.12*b*) yield $u_z \sim 1/\delta$, $E_\theta \sim R \sim \delta$ inside the jet. Taking into account these estimations and making use of (1.2*b*), (2.8), and (2.9), one can readily verify that $\tau_e/\tau_h \to \infty$ as $\delta \to 0$, where $\tau_e \sim \sigma^\circ/(K\tilde{E}_\theta)$ is the electric relaxation time for the jet and $\tau_h \sim L/\tilde{u}_z$ is its hydrodynamic time. Here, $\tilde{u}_z = u^\circ u_z$ and $\tilde{E}_\theta = E^\circ E_\theta$ are the dimensional components of the liquid velocity and electric field inside the jet; E° and u° are defined by (2.8).

5. Asymptotic analysis of the outer region

To obtain more detailed information on the structure of the meniscus and jet, one has to solve equations (4.10)–(4.19), (4.23)–(4.26).

5.1. *Electric field and liquid velocity inside the meniscus*

The remarkable feature of the leading perturbation is the fact that equations (4.10)–(4.19) allow one to obtain the electric field distribution in V_m without finding the liquid velocity. Indeed, their 'electrical' part (see (4.10), (4.13*c*), (4.16*a*), and (4.17*a*)) is independent of the liquid flow and can be readily solved:

$$\phi_{m1} = -\frac{Af}{\epsilon r}, \ \boldsymbol{D}_{m1} = \epsilon \boldsymbol{E}_{m1} = -\frac{Af\boldsymbol{r}}{r^3} \ \text{ in } \ V_m \ \left(A \equiv \frac{1}{2\pi(1-\cos\alpha)} = 0.46\right). \tag{5.1a,b}$$

The flow in V_m is governed by the Stokes equations (4.11*b*) with boundary conditions

(4.14) in which $\boldsymbol{D}_{m1}$ is known and determined by (5.1*b*). Given (4.11*a*) at $k = 1$, the components of vector $\boldsymbol{U}_1$ can be expressed in terms of the stream function $\psi(r, \theta)$:

$$U_{1r} = \frac{-1}{r^2 \sin\theta} \frac{\partial \psi}{\partial \theta}, \quad U_{1\theta} = \frac{1}{r \sin\theta} \frac{\partial \psi}{\partial r}, \tag{5.2a,b}$$

where ψ is regular at $\theta = 0$. The functions ψ and P_1 satisfy the linear differential equations (Happel & Brenner 1965)

$$\hat{\mathrm{D}}^2 \psi = 0 \quad \left(\hat{\mathrm{D}} \equiv \frac{\partial^2}{\partial r^2} + \frac{\sin\theta}{r^2} \frac{\partial}{\partial \theta} \frac{1}{\sin\theta} \frac{\partial}{\partial \theta} \right), \tag{5.3}$$

$$\frac{\partial P_1}{\partial r} = \frac{-1}{r^2 \sin\theta} \frac{\partial \hat{\mathrm{D}} \psi}{\partial \theta}, \quad \frac{\partial P_1}{\partial \theta} = \frac{1}{\sin\theta} \frac{\partial \hat{\mathrm{D}} \psi}{\partial r}, \tag{5.4a,b}$$

which follow from (5.2) and (4.11*b*) at $k = 1$. Substituting (5.2) into (4.14*a*,*b*) and (4.16*b*), taking into account (2.25*b*), (5.1*b*), and making use of the regularity requirements at $\theta = 0$, we derive the boundary conditions to equations (5.3), (5.4):

$$\psi = 0, \quad \frac{\partial}{\partial \theta} \frac{1}{\sin\theta} \frac{\partial \psi}{\partial \theta} = B f r^{1/2} \quad \text{at} \quad \theta = \alpha \quad \left(B \equiv \frac{(2/\tan\alpha)^{1/2}}{2\pi(1 - \cos\alpha)} = 0.60 \right); \tag{5.5a,b}$$

$$\psi = 0, \quad \frac{\partial \psi}{\partial \theta} = 0 \quad \text{at} \quad \theta = 0. \tag{5.6a,b}$$

The solution that satisfies (5.3)–(5.6) and (4.17*b*) is obtained in the Appendix and given by

$$\psi = \frac{B f r^{1/2} \sin\theta}{4} \left(\frac{P'_{-1/2}(\cos\theta)}{P'_{-1/2}(\cos\alpha)} - \frac{P'_{3/2}(\cos\theta)}{P'_{3/2}(\cos\alpha)} \right), \quad P_1 = -\frac{3 B f P_{3/2}(\cos\theta)}{2 r^{5/2} P'_{3/2}(\cos\alpha)}, \tag{5.7a,b}$$

where $P_{-1/2}$ and $P_{3/2}$ are the standard Legendre functions of degree $-1/2$ and $3/2$, respectively, and primes denote the derivatives with respect to θ. The stream function (5.7*a*) describes a fluid circulation induced by the electrical shear stress at the surface of the conical meniscus. The liquid moves towards its apex along generatrices and returns back along the meniscus axis. Such flows inside Taylor cones are observed in numerous experiments (Hayati, Bailey & Tadros 1986, 1987). Finally, (4.11) at $k = 2$, (4.14*c*,*d*), (4.16*c*), and (4.17*c*) yield the velocity and pressure of the sink flow of an inertialess fluid for U_2 and P_2:

$$U_{2r} = -\frac{A}{r^2}, \quad U_{2\theta} = 0, \quad P_2 = 0 \quad (A = 0.46), \tag{5.8a–c}$$

where A is the constant defined by (5.1).

Substituting (5.2) and (5.8) into expansion (4.1) for $\boldsymbol{u}$, taking into account (4.7*b*) and (5.7*a*) and making necessary evaluations one can find the non-dimensional velocity $\boldsymbol{u}$ at any point inside the meniscus domain V_m. For example, the values of u_r at the surface Σ_m ($\theta = \alpha + \delta\Theta_1$) and semiaxis $z < 0$ ($\theta = 0$) are given by (see the Appendix)

$$u_r|_{\Sigma_m} = -0.146 \frac{\delta^{2/3} f}{\epsilon Ca\, r^{3/2}} - 0.46 \frac{\delta}{r^2}, \quad u_r|_{\theta=0} = 0.154 \frac{\delta^{2/3} f}{\epsilon Ca\, r^{3/2}} - 0.46 \frac{\delta}{r^2}. \tag{5.9a,b}$$

Figure 2(*a*) shows a qualitative pattern of streamlines of the $\boldsymbol{u}$-field mentioned above. The most interesting feature is a stagnation point located at the symmetry axis at

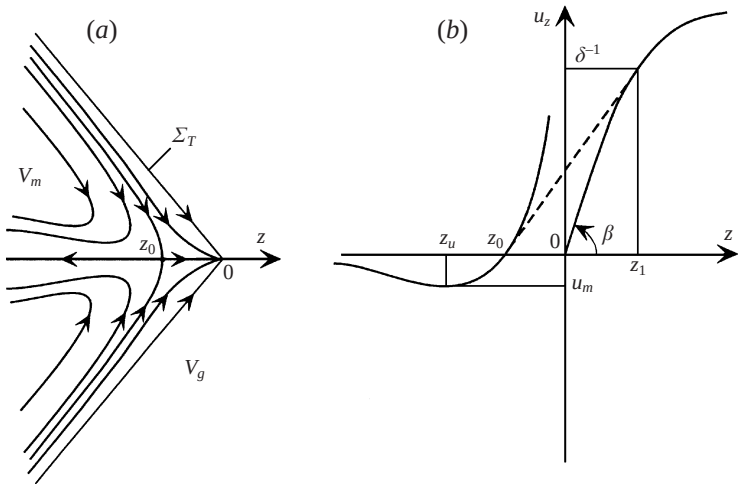

FIGURE 2. The streamlines of the $\boldsymbol{u}$-field at $\theta \leqslant \alpha$ (a) and the liquid velocity u_z at the meniscus-jet axis (b). The solid lines in (b) demonstrate the behaviour of the first-order solution: $u_z = -u_r(r)$ at $z < 0$ and $u_z = U_j/\delta$ at $z > 0$, where u_r and U_j are determined by (5.9b) and (5.12). Dependences of the characteristic coordinates z_0, z_u, u_m on the parameters δ, Ca, f, ϵ are given by (5.10) and (5.11); $z_1 = 1.75(0.28 + \Gamma/f)^2$, $\tan\beta = 0.57f^2/(\delta\Gamma^2)$. The dashed line in ($b$) shows the linear interpolation of the liquid velocity over the transition region.

$z = z_0$, where z is the axial coordinate defined in § 2 and z_0 is given by

$$z_0 = -8.87\delta^{2/3}\left(\frac{\epsilon Ca}{f}\right)^2. \tag{5.10}$$

It should be recalled here that the meniscus and jet characteristics scale in different ways (see (4.1)–(4.4)). As a result, if we want to compare their behaviour, it is more convenient to use qualitative representations rather than plots calculated for some fixed values of δ, Ca, f, ϵ, Γ. For example, the behaviour of the function $u_z(z) \equiv -u_r(r,0)$ along the meniscus axis $\theta = 0$ is shown in figure 2(b) (the solid line at $z < 0$), $u_r(r,0)$ being given by (5.9b) with $r = -z$. The liquid moves back from the apex at $z < z_0$ (z_0 is defined by (5.10)). The magnitude of the backward flow velocity has the maximum $|u_m|$ at $z = z_u$, where

$$u_m = -0.001\delta^{-1/3}\left(\frac{f}{\epsilon\, Ca}\right)^4, \quad z_u = -15.77\delta^{2/3}\left(\frac{\epsilon Ca}{f}\right)^2. \tag{5.11a,b}$$

The points with coordinates $z = z_0$ and $z = z_u$ belong to the transition region if $(\epsilon Ca/f)^2$ is of the order of , or smaller than 10^{-1}. In this case, relations (5.10) and (5.11) can only provide quantitative estimates for z_0, z_u and u_m.

It is worth noting that, although the small parameter δ is proportional to the liquid density ρ, the latter does not affect dimensional distributions of the electric potential, velocity, and pressure inside the meniscus, to the leading order. Indeed, according to (2.8) and (2.9), the quantities L, ϕ°, u°, and p° which appear in the definitions of non-dimensional variables (2.6), (2.7) are proportional to $\rho^{-2/3}$, $\rho^{-1/3}$, $\rho^{1/3}$, and $\rho^{2/3}$, respectively. The functions ϕ_{m1}, $\boldsymbol{U}_1$, P_1, and $\boldsymbol{U}_2$ determined by (5.1), (5.2), (5.7), and (5.8) are again proportional to r^{-1}, $r^{-3/2}$, $r^{-5/2}$, and r^{-2}, respectively, where $r \equiv \tilde{r}/L$. As a result, a dimensional form of the solutions obtained for the electric potential, velocity, and pressure does not depend on the liquid density. Obviously,

the liquid viscosity μ affects, to the leading order, only the velocity distribution inside the meniscus. Indeed, the definitions of non-dimensional variables (2.6), (2.7) do not contain the liquid viscosity. It appears only in definition (1.3*a*) for the capillary number Ca. The latter, in turn, affects only the asymptotic expansion (4.1) for the liquid velocity.

5.2. *Characteristics of the jet*

Integrating (4.23), we have

$$\frac{1}{2}U_j^2 + \frac{\Gamma}{f}(\pi U_j)^{1/2} = 2C_\tau z^{1/2}. \tag{5.12}$$

Generally speaking, an arbitrary additive constant could appear in (5.12). However, such a constant should be omitted as we consider the leading perturbation in the jet domain. Indeed, the jet velocity $u_z = U_j/\delta$ should be matched with the velocity in the transition domain V_t, where $r \sim r^*/L \equiv \delta^{2/3}$ and $u_z \sim \delta^{-1/3}$ due to (2.20*b*). As a result, $U_j \sim \delta^{2/3}$ at $z \sim \delta^{2/3}$, and both sides of (5.12) turn out to be of the order of $\delta^{1/3}$ at $z \sim \delta^{2/3}$. Hence, the arbitrary constant in (5.12) would be of the order of $\delta^{1/3}$ as well and must vanish as $\delta \to 0$. The relationship (5.12) determines the function $U_j(z)$ in the implicit form and yields the following asymptotics for $U_j(z)$:

$$U_j = \frac{4C_\tau^2 f^2}{\pi\Gamma^2} z + o(z) \quad \text{as} \quad z \to 0, \quad U_j = 2C_\tau^{1/2} z^{1/4} + o(1) \quad \text{as} \quad z \to \infty. \tag{5.13a,b}$$

The behaviour of the function $u_z = U_j/\delta$ along the jet is shown in figure 2(*b*) (the solid line at $z > 0$). Evidently, the velocity distribution $u_z(z)$ represented by solid lines in figure 2 is not valid at sufficiently small $|z|$, which indicates that outer expansions (4.1)–(4.4) fail in the transition region.

The exact explicit expression for $U_j(z)$ can be obtained from (5.12) as a solution by radicals. Unfortunately, it is too bulky and cannot be used directly in the subsequent asymptotical analysis. For this reason, one has to employ approximate analytical expressions for $U_j(z)$ whose asymptotics, however, must coincide with equations (5.13). One of the simplest such expressions is given by

$$U_j = \frac{4C_\tau^2 f^2 z}{\pi\Gamma^2 + 2C_\tau^{3/2} f^2 z^{3/4}} \tag{5.14}$$

with a relative error of several per cent (depending on values of f and Γ) for finite z. It is also worth noting that the asymptotic expansions for (5.14) coincide with those for the exact U_j-expression only to the leading order. Thus, applying expression (5.14) as $z \to 0$ or $z \to \infty$, we can use no additional terms in asymptotic expansions for (5.14) but only the leading ones.

As $U_j(z)$ is known, equations (4.24) immediately yield P_j, R_j, q_j, σ_j in terms of $U_j(z)$:

$$P_j = \Gamma(\pi U_j)^{1/2}, \quad R_j = \frac{1}{(\pi U_j)^{1/2}}, \quad q_j = \frac{f}{U_j}, \quad \sigma_j = \frac{f}{2(\pi U_j)^{1/2}}. \tag{5.15a–d}$$

It should be observed that (5.15*b,c*) automatically satisfy limiting conditions (4.26). Finally, substituting (5.15) into (4.4), we obtain all the characteristics of the jet, to the leading order, except for the electric potential. To find it, we should examine the electric field distribution in the surrounding gas.

5.3. *Electric field in the gas domain; meniscus shape*

The functions ϕ_{g1}, $\boldsymbol{E}_{g1}$ in the asymptotic expansion (4.3) for electric field in the gas domain V_g satisfy the equations

$$\nabla^2\phi_{g1} = 0, \quad \boldsymbol{E}_{g1} = -\nabla\phi_{g1}, \tag{5.16a,b}$$

which follow from (4.12). Substituting the expressions (2.25*b*) and (5.1*a*) for σ_T and ϕ_{m1} into (4.13*a*), we obtain the following boundary condition to (5.16*a*) at the meniscus surface:

$$\phi_{g1} - \left(\frac{2r}{\tan\alpha}\right)^{1/2}\Theta_1 = -\frac{Af}{\epsilon r} \quad \text{at} \quad \theta = \alpha, \tag{5.17}$$

where A is the constant defined by (5.1). Condition (5.17) contains the unknown function $\Theta_1(r)$; therefore one more equation at $\theta = \alpha$ is required. To formulate it, we should calculate the left-hand side of (4.15) using the derived distributions of the velocity and pressure in the meniscus (see the Appendix). Substituting (A 14) into (4.15) and taking into account expressions (2.25*b*) and (5.16*b*) for σ_T and $\boldsymbol{E}_{g1}$, we have

$$\frac{Cf}{\epsilon r^{5/2}} = \left(\frac{2}{\tan\alpha}\right)^{1/2}\frac{1}{r^{3/2}}\frac{\partial\phi_{g1}}{\partial\theta} + \frac{\Theta_1}{r\tan^2\alpha} - \frac{1}{r}(r(r\Theta_1)')' \quad \text{at} \quad \theta = \alpha, \tag{5.18}$$

where C is the constant given by (A 16). Finally, there are two more asymptotic conditions (4.25), which take into account the jet charge. Substituting (5.15*c*) into (4.25*b*), using the approximation (5.14) for $U_j(z)$, and recalling that $z = r$ at $\theta = \pi$, we obtain

$$2\pi\sin\theta\frac{\partial\phi_{g1}}{\partial\theta} \to \frac{\pi\Gamma^2}{4C_T^2 f r} + \frac{f}{2C_T^{1/2}r^{1/4}} \quad \text{as} \quad \theta \to \pi, \tag{5.19}$$

where C_T is the constant determined by (2.5*b*). If the exact value of $U_j(z)$ following from (5.12) was used in (5.15*c*), the right-hand side of (5.19) would become much more cumbersome. In this case we still could generalize the subsequent analysis making use of the Mellin transform. Such generalization would have no effect on the asymptotic behaviour of the meniscus-jet characteristics at small and large r. However, it would greatly complicate the consideration by involving the Legendre functions of complex degrees.

We shall seek the solution to the problem (5.16*a*), (5.17)–(5.19) in the form

$$\phi_{g1} = r^{-1}L_{-1}(\cos\theta) + r^{-1/4}L_{-1/4}(\cos\theta), \quad \Theta_1 = C_1 r^{-3/2} + C_2 r^{-3/4}, \tag{5.20a,b}$$

where C_1 and C_2 are constant, L_{-1} and $L_{-1/4}$ are general solutions to the Legendre equations of degrees -1 and $-1/4$, respectively, to which (5.16*a*) is reduced by substitution (5.20). As a result, (5.20) will satisfy the Laplace equation (5.16*a*). Obviously, (5.20) also automatically satisfy the limiting conditions (4.18*b*) and (4.19) as $r \to \infty$. Functions L_{-1} and $L_{-1/4}$ can be represented as the linear combinations of the particular solutions of the Legendre equations (Abramovitz & Stegun 1964):

$$L_{-1} = A_1 + B_1\ln\frac{1+\cos\theta}{1-\cos\theta}, \quad L_{-1/4} = A_2 P_{-1/4}(-\cos\theta) + B_2 P_{-1/4}(\cos\theta), \tag{5.21a,b}$$

where A_1, B_1, A_2, B_2 are constant, and $P_{-1/4}(\cos\theta)$ is the standard Legendre function which is regular at $\theta = 0$ and logarithmically singular at $\theta = \pi$:

$$P_{-1/4}(\cos 0) = 1, \quad P_{-1/4}(\cos\theta) \to -\frac{\sqrt{2}}{\pi}\ln(\pi-\theta) + \text{const.} \quad \text{as} \quad \theta \to \pi. \tag{5.22a,b}$$

It follows from (5.22) that $P_{-1/4}(\cos\theta)$ and $P_{-1/4}(-\cos\theta)$ are linearly independent. To find the unknown constants in (5.20*b*) and (5.21), let us replace the functions L_{-1} and $L_{-1/4}$ in (5.20*a*) by their expressions (5.21) and then substitute (5.20) into conditions (5.17)–(5.19), taking into account (5.22). As a result, (5.19) yields

$$B_1 = -\frac{\Gamma^2}{16C_T^2 f} = -0.14\frac{\Gamma^2}{f}, \quad B_2 = \frac{f}{4(2C_T)^{1/2}} = 0.22f, \tag{5.23a,b}$$

and (5.17), (5.18) are reduced to the system of linear algebraic equations for A_1, A_2, C_1, C_2. After straightforward calculations, we obtain its solution

$$A_1 = 0.74\frac{f}{\epsilon} - 1.06\frac{\Gamma^2}{f}, \quad A_2 = -1.47f, \tag{5.24a,b}$$

$$C_1 = 0.92\frac{f}{\epsilon} - 0.97\frac{\Gamma^2}{f}, \quad C_2 = -1.34f, \tag{5.25a,b}$$

where we have used expressions (5.1) and (A16) for the constants A and C and evaluated all the coefficients that depend only on π and $\alpha = 49.29°$.

Now we are able to find the term $\Delta_\phi(\delta)\Phi$ in expansion (4.4) for the electric potential of the jet. Substituting (5.20*a*) into (4.25*a*) and taking into account (5.21)–(5.23), we obtain, to the leading order,

$$\Delta_\phi = -\delta\ln\delta, \quad \Phi = \frac{\Gamma^2}{8C_T^2 f z} + \frac{f}{4\pi C_T^{1/2} z^{1/4}}. \tag{5.26a,b}$$

This expression for Φ coincides with the right-hand side of (5.19) divided by 2π, which is not surprising since the asymptotic conditions (4.25) yield

$$\Delta_\phi(\delta)\Phi = -(\delta\ln\delta)\frac{q_j}{2\pi} \tag{5.27}$$

for any function $\phi_{g1}(r,\theta)$ that is logarithmically singular as $\theta \to \pi$.

Relations (5.20)–(5.25) and (5.26*b*) determine the (scaled) leading perturbations of the latitude (at the meniscus surface) and electric potential (in the surrounding gas and along the jet). Using them in the asymptotic expansions (4.2)–(4.4) and taking into account the basic solution (4.8*b*), (4.9), we can calculate the total potential of the jet:

$$\phi = -2C_T z^{1/2} - (\delta\ln\delta)\left(\frac{\Gamma^2}{8C_T^2 f z} + \frac{f}{4\pi C_T^{1/2} z^{1/4}}\right) \quad \text{at} \quad z > 0, \tag{5.28}$$

and the meniscus shape (in the spherical coordinates):

$$\theta = \Theta(r), \quad \Theta = \alpha + \delta\left(C_1 r^{-3/2} + C_2 r^{-3/4}\right), \tag{5.29a,b}$$

where the coefficients C_1, C_2 are determined by (5.25). The dependence of the meniscus radius R on the axial coordinate z is expressed in the parametric form as follows:

$$R = r\sin\Theta(r), \quad z = -r\cos\Theta(r) \quad \text{at} \quad \Sigma_m, \tag{5.30a,b}$$

where the function $\Theta(r)$ is given by (5.29*b*) and r can be treated as a parameter. On the other hand, substituting (4.7*a*), (5.1*a*), and (5.15*b*) into expansions (4.1), (4.4) and making use of (5.14), we readily obtain the electric potential at the meniscus symmetry axis and the jet radius:

$$\phi = \frac{\delta A f}{\epsilon z} \quad \text{at} \quad z < 0, \quad R = \delta\left(\frac{\Gamma^2}{4C_T^2 f^2 z} + \frac{1}{2\pi C_T^{1/2} z^{1/4}}\right)^{1/2} \quad \text{at} \quad \Sigma_j. \tag{5.31a,b}$$

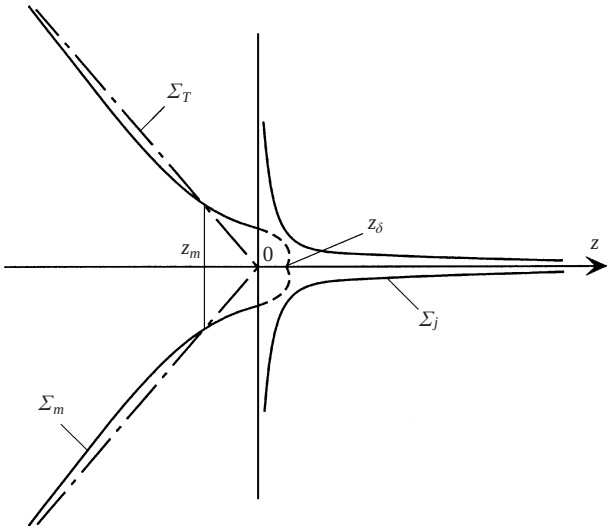

FIGURE 3. The meniscus-jet shape. The solid lines show, to the leading order, the meniscus and jet profiles which follow from (5.29) and (5.31*b*). The dashed-dotted line corresponds to Taylor's cone of semiangle $\alpha = 49.29°$. The dashed line extrapolates the meniscus profile determined by (5.29) into the transition region. Dependences of the characteristic coordinates z_m and z_δ on the parameters δ, f, ϵ, Γ are given by (5.32) and (6.2).

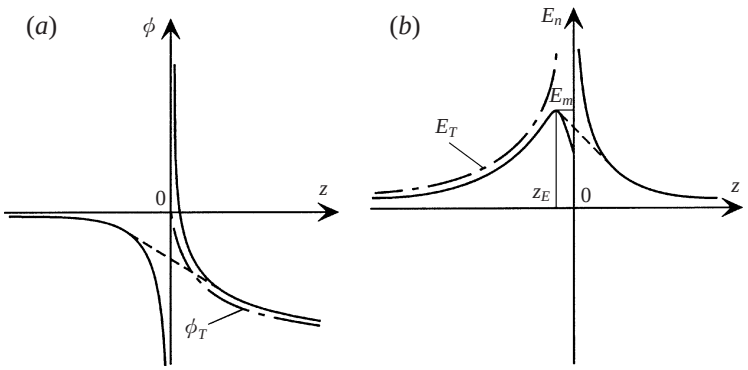

FIGURE 4. The electric potential (*a*) and the normal component of the outer electric field at the meniscus-jet surface (*b*). The solid lines demonstrate the behaviour of the first-order solutions $\phi(z)$, $E_n(z)$ which are determined by (5.31*a*), (5.33) for the meniscus and by (5.28), (5.36) for the jet. The dashed-dotted lines show Taylor's potential at the semiaxis $\theta = \pi$ (*a*) and the value of E_n at the surface of Taylor's cone with no jet (*b*). Dependences of the characteristic coordinates E_m and z_E on the parameters δ, f, ϵ, Γ are given by (5.35). The dashed lines show the linear interpolation of the electric potential and normal electric field over the transition region.

Figure 3 demonstrates the meniscus-jet shape which follows from (5.29) (or (5.30)) and (5.31*b*). The solid lines at $z < 0$ and $z > 0$ show the meniscus and jet profile, respectively. The dashed-dotted lines demonstrate the profile of Taylor's cone. It should be observed that the meniscus surface latitude Θ is a little less than Taylor's angle α at $z < z_m$ and larger than α at $z > z_m$, where

$$z_m = -\left(\frac{0.50}{\epsilon} - \frac{0.53\Gamma^2}{f^2}\right)^{4/3}. \tag{5.32}$$

Figure 4(*a*) shows the electric potential distribution (solid lines) which is determined by (5.28) and (5.31*a*) at the meniscus-jet axis. The dashed-dotted line demonstrates Taylor's potential at the semiaxis $z > 0$, which is given by (2.25*a*) at $\theta = \pi$. Obviously, the potential distribution obtained is not valid inside a sufficiently small vicinity of the point $z = 0$. As before, this fact indicates a failure of the outer expansions (4.1)–(4.4) in the transition region.

5.4. *Meniscus-jet surface charge*

Let us now find the meniscus surface charge density σ and the normal component E_n of the electric field strength at the meniscus surface. The boundary condition (2.14*b*) for $\boldsymbol{E}$ and asymptotic expansion (4.2) for σ with allowance for (4.8*a*) and (2.25*b*) yield

$$E_n \equiv \boldsymbol{n} \cdot \boldsymbol{E}_g = \sigma, \quad \sigma = \left(\frac{2}{r \tan \alpha}\right)^{1/2} + \delta\sigma_1(r) \ \text{ at } \ \Sigma_m, \tag{5.33a,b}$$

because the normal electric field inside the meniscus vanishes to the leading order (see (4.7*a*) and (4.13*c*)). The right-hand sides of (5.33*a*, *b*) are completely determined if the (scaled) meniscus charge perturbation σ_1 is known. Substituting (5.20) into (4.13*b*), making use of (5.21), (5.23)–(5.25), and calculating all the coefficients that depend only on α, we obtain

$$\sigma_1 = -\left(1.04\frac{f}{\epsilon} - 0.74\frac{\Gamma^2}{f}\right)\frac{1}{r^2} + 0.82\frac{f}{r^{5/4}} \ \text{ at } \ \Sigma_m. \tag{5.34}$$

Relations (5.33), (5.34) together with (5.30*b*) yield the dependence $E_n(z)$ in a parametric form if r is regarded as a parameter. Figure 4(*b*) shows the distribution of the normal electric field E_n along the meniscus generatrix (the solid line at $z < 0$). The dashed-dotted line demonstrates Taylor's value of E_n given by (2.25*b*). The function $E_n(z)$ has its maximum E_m at $z = z_E$, where

$$E_m = \frac{1}{\delta^{1/3}}\left(3.32\frac{f}{\epsilon} - 2.36\frac{\Gamma^2}{f}\right)^{-1/3}, \quad z_E = \frac{-0.97}{E_m^2}\cos\frac{1.15f^2 - 0.92\Gamma^2\epsilon}{f^2 - 0.71\Gamma^2\epsilon}, \tag{5.35a,b}$$

to the leading order. This fact indicates that the normal electric field reaches its maximum in the transition region. Finally, the distribution of the surface charge and normal electric field along the jet follows from (4.3), (4.4), (4.25*b*), and (5.15):

$$E_n = \sigma = \frac{1}{2}\left(\frac{\Gamma^2}{4C_T^2 z} + \frac{f^2}{2\pi C_T^{1/2} z^{1/4}}\right)^{1/2} \ \text{ at } \ \Sigma_j. \tag{5.36}$$

In deriving (5.36), we have used (5.14) and taken into account that the strength of Taylor's field is parallel to the jet surface in the limit $\delta \to 0$. The behaviour of the function (5.36) is shown by the solid line in figure 4(*b*) at $z > 0$. It should be observed that values of E_n and σ at the jet surface do not depend on δ and therefore do not vanish as $\delta \to 0$. However, the total charge per unit length of the jet vanishes and so does the jet vicinity in which the non-vanishing component E_θ is concentrated since the jet radius is proportional to δ (see (5.31*b*)).

Evidently, the liquid viscosity affects no characteristics of the jet, meniscus surface or electric field, to the leading order. Indeed, the capillary number Ca does not appear in the asymptotic equations (and solutions) for the jet, electric field, and meniscus surface. In contrast, the liquid density affects the velocity, pressure, radius and charge of the jet because its velocity equation (5.12) contains the inertial term. As a result, the electric field in the surrounding gas as well as the surface charge and shape of

the meniscus depend on the liquid density. However, its effect vanishes as $r \to 0$, i.e. in the vicinity of the transition region because the first (inertial) term in equation (5.12) becomes negligible at sufficiently small z. In this case, the asymptotics of the jet characteristics are given by (5.13*a*) and (5.15), and the asymptotics of the electric field, meniscus shape, and surface charge are determined by the first terms on the right-hand side of (5.20) and (5.34). Using the definitions of the small parameter δ and non-dimensional variables (see (1.9) and (2.6)–(2.9)), one can readily verify that the asymptotic behaviour (as $r \to 0$) of the dimensional characteristics of the jet, electric field, and meniscus surface does not depend on the liquid density, to the leading order.

It is also worth noting that we have ignored, in accordance with the singular perturbation theory (Van Dyke 1975), the so-called eigensolutions which could be added to expressions obtained for ϕ_{m1}, $\boldsymbol{U}_1$, P_1, ϕ_{g1}, Θ_1. Obviously, such eigensolutions should be regular (at $\theta = \pi$) solutions to the uniform problem which results from (4.10)–(4.19) by putting $f \equiv 0$. Some of them are more singular (at $r = 0$) than ϕ_{m1}, $\boldsymbol{U}_1$, P_1, ϕ_{g1}, Θ_1 and can be eliminated by asymptotic matching with the solution in the transition region. The others would result in redetermining the basic solution (4.7)–(4.9).

6. Qualitative analysis of the transition region

As we have already noted, the outer expansions fail in a sufficiently small vicinity of the virtual apex, because perturbations grow as $r \to 0$. The leading perturbation equations and solutions obtained from them show that the perturbations stop being relatively small at $r \sim \delta^{2/3}$, i.e. in the transition region. As a result, we should rescale the outer non-dimensional variables to adapt them to studying that region:

$$\left.\begin{array}{l} r = \delta^{2/3} r_t, \quad R = \delta^{2/3} R_t, \quad U = \delta^{-1/3} U_t, \quad p = \delta^{-2/3} p_t, \\ \phi = \delta^{1/3} \phi_t, \quad \boldsymbol{E} = \delta^{-1/3} \boldsymbol{E}_t, \quad \boldsymbol{D} = \delta^{-1/3} \boldsymbol{D}_t, \quad \sigma = \delta^{-1/3} \sigma_t. \end{array}\right\} \tag{6.1}$$

Such rescaling corresponds to passing from the outer spatial scale L to the transition region scale r^* in definitions (2.6)–(2.8). Substituting (6.1) into (2.11)–(2.20) and putting $\delta \to 0$, one can obtain the system of governing equations which determine the (scaled) variables in the transition region and no longer depend on δ. As a result, the quantities with subscript t in (6.1) do not depend on δ; therefore expression (6.1) provide true scaling in the transition region for the variables defined by (2.6)–(2.8).

Rigorous asymptotic analysis of that region requires separate studies and will be the subject of another publication. Below, we shall consider only quantitative estimations for the behaviour of the variables in the transition region, which would be enough for many applications. The asymptotic solution in the transition region should be matched with the meniscus and jet solutions, i.e. the solutions in the meniscus and jet domains, found in § 5. This fact suggests that we could obtain some useful qualitative information about the transition region by interpolating the meniscus-jet solution over that region or extrapolating the meniscus and jet solutions into the transition region. The dashed line in figure 3 shows the result of the extrapolation of the solution obtained for the meniscus profile. Obviously, such a procedure is possible only for $\Theta \leqslant \pi$ since the extrapolated meniscus radius vanishes at $\Theta = \pi$ in accordance with (5.30*a*). This fact comes as no surprise, as the flow rate through the meniscus vanishes, to the leading order. It appears only in the next approximation that contains the term $\delta \boldsymbol{U}_2$ in the velocity expansion (4.1) (see (4.16*b*,*c*)). Using (5.30*b*), (5.29*b*), and (5.25*a*),

we readily obtain, to the leading order,

$$z_\delta = \left(\frac{\delta C_1}{\pi - \alpha}\right)^{2/3} = \delta^{2/3}\left(0.40\frac{f}{\epsilon} - 0.43\frac{\Gamma^2}{f}\right)^{2/3}, \tag{6.2}$$

where z_δ is the maximum length of the meniscus profile extrapolation into the transition region (see figure 3) and $\alpha = 0.27\pi$.

Examples of the linear interpolation for the liquid velocity, electric potential, and normal electric field strength are demonstrated by the dashed straight lines in figures 2(*b*) and 4(*a,b*), respectively. These lines are tangent to the solid ones that show the solutions for the meniscus and jet regions and are uniquely determined by them. Interpolation accuracy can be improved by using the cubic interpolation for the electric potential and the quadric one for the electric field strength. We shall not dwell on this in detail, as the method in question is clear from a theoretical point of view, though final interpolation expressions are too cumbersome.

The quantity z_δ provides an effective scale for the transition liquid domain V_{tl}. Since the jet domain V_j continuously turns into V_{tl}, the condition of the jet thinness ($R \ll z$ in V_j) must be violated at $z \simeq z_\delta$, which implies the relationship $R(z_\delta) \simeq z_\delta$. Substituting expressions (5.31*b*) and (6.2) for R and z_δ into this relationship, we obtain, to the leading order,

$$\frac{\Gamma}{2C_T f}\left(0.40\frac{f}{\epsilon} - 0.43\frac{\Gamma^2}{f}\right)^{-1/3} \simeq \left(0.40\frac{f}{\epsilon} - 0.43\frac{\Gamma^2}{f}\right)^{2/3}. \tag{6.3}$$

Recalling that $C_T = 0.67$ and solving (6.3) with respect to f, we find

$$f \simeq f_{th}(\epsilon, \Gamma), \quad \text{where} \quad f_{th} = (1.87\Gamma + 1.07\Gamma^2)^{1/2}\epsilon^{1/2}. \tag{6.4a,b}$$

Substituting definition (1.6) for f into (6.4*a*), we obtain the scaling law (1.1)

$$I \simeq f_{th}(\epsilon, \Gamma)\left(\frac{\gamma K Q}{\epsilon}\right)^{1/2}, \tag{6.5}$$

with the theoretical coefficient given by (6.4*b*). The function $f_{th}(\epsilon)$ determined by (6.4*b*) at $\Gamma = 1,\ 1.2$ is shown by solid lines in figure 5 (curves 1*a* and 2*a*). Although we have used qualitative analysis, the theoretical value $f_{th}(\epsilon)$ conforms fairly well to the experimental data (Fernández de la Mora & Loscertales 1994; Chen & Pui 1997) which are shown by the dashed lines in figure 5.

The scaling law (6.5) can be also derived in a different way. To do that, we shall use the following remarkable feature of the main terms of the asymptotic expansions for the electric potential distribution along the meniscus and jet surfaces. These terms can be rewritten in a similar way:

$$\phi = -\frac{\delta A f}{\epsilon r} + \cdots = -\frac{\delta A f \sin\alpha}{\epsilon R} + \cdots \qquad \text{at} \quad \Sigma_m, \tag{6.6a}$$

$$\phi = -2C_T z^{1/2} + \cdots = -\frac{\delta\Gamma}{fR} + \cdots \qquad \text{at} \quad \Sigma_j, \tag{6.6b}$$

where we have used expressions (4.1), (5.1*a*), and (5.30*a*) for the meniscus potential and radius, as well as expressions (5.28) and (5.31*b*) for the jet potential and radius (in the limit $\delta \to 0$). Extrapolating the main terms of asymptotic expansions (6.6*a,b*) into the transition region, we come to the conclusion that they can be matched only

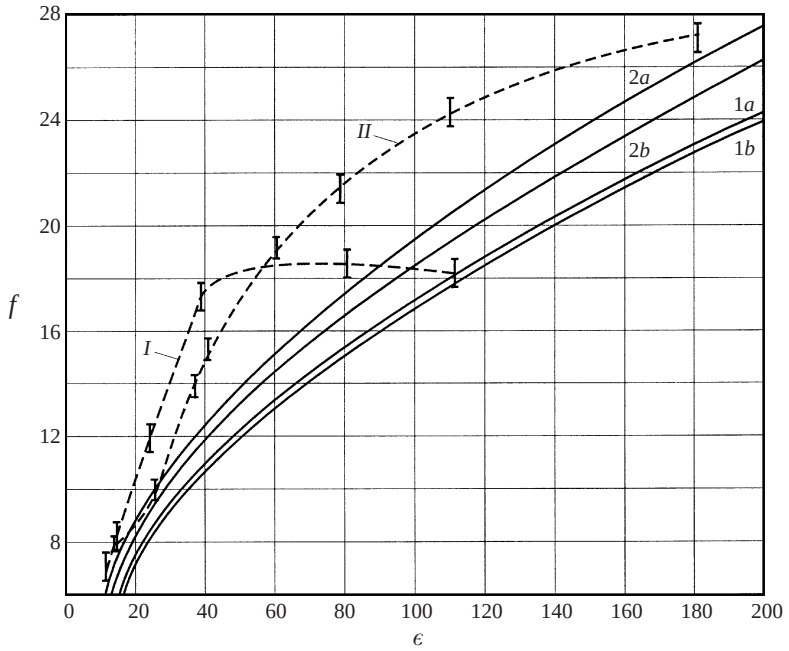

FIGURE 5. The non-dimensional current f as a function of the dielectric constant ϵ for $\Gamma = 1$ (curves 1) and $\Gamma = 1.2$ (curves 2). Lines marked with a and b correspond to the theoretical values $f_{th}(\epsilon)$ calculated from (6.4b) and (6.8b), respectively. Experimental data $f_{exp}(\epsilon)$ are shown by the dashed lines I (Fernández de la Mora & Loscertales 1994) and II (Chen & Pui 1997).

if

$$\frac{Af\sin\alpha}{\epsilon} = \frac{\Gamma}{f}, \quad \text{where} \quad A \equiv \frac{1}{2\pi(1-\cos\alpha)}. \tag{6.7}$$

Solving (6.7) with respect to f and calculating the coefficient which depends only on α, we have

$$f = f_{th}(\epsilon,\ \Gamma), \quad \text{where} \quad f_{th} = 1.69(\Gamma\epsilon)^{1/2}. \tag{6.8a,b}$$

The function $f_{th}(\epsilon)$ determined by (6.8b) at $\Gamma = 1,\ 1.2$ is shown by solid lines in figure 5 (curves 1b, 2b) and is also consistent with the experimental data represented by the dashed lines. It is worth noting that at $\Gamma = 1$ expressions (6.4b) and (6.8b) yield almost the same values, $f_{th} = 1.71\epsilon^{1/2}$ and $f_{th} = 1.69\epsilon^{1/2}$, respectively.

It should also be observed that relations (2.6), (2.9), and (5.31b) yield, to the leading order, the following estimation for the dimensional radius of the jet near its head:

$$R^* \sim LR\Big|_{z\sim\delta^{2/3}} = \frac{\Gamma r^*}{2C_T f}. \tag{6.9}$$

This relation is consistent with (1.2) since $\Gamma/(2C_T f) \sim 0.1$.

Let us also estimate the electric field in the transition region. Using the extrapolation and interpolation methods mentioned above, we obtain the normal electric field distribution along the liquid surface inside the transition region. In particular, the maximum value of the normal electric field can be estimated by means of (5.35a). Another practically interesting characteristic is the electric field flux Ω through an arbitrary surface $\Sigma_0(r = \delta^{2/3}r_t,\ \alpha < \theta < \pi)$ which is located inside the gas subdomain

of the transition region:

$$\Omega(r_t) \equiv \int_{\Sigma_0} (\boldsymbol{E} \cdot \boldsymbol{N}_0) \mathrm{d}\Sigma_0 = \delta\Omega_0 + o(\delta) \quad \text{as} \quad \delta \to 0, \tag{6.10}$$

where $\boldsymbol{N}_0$ is the normal to Σ_0 and Ω_0 is the leading term of the asymptotic expansion of Ω. Finding the electric field strength from (4.3), (4.9), (5.20*a*), and (5.21), extrapolating it into the transition region, and calculating the integral (6.10), we obtain

$$\Omega_0 = 4.17 r_t^{3/2} + 7.72 \frac{f}{\epsilon} - 10.22 \frac{\Gamma^2}{f}. \tag{6.11}$$

The quantity r_t, which appears in the definition of Σ_0 and relation (6.11), should satisfy the inequalities

$$\left(0.40 \frac{f}{\epsilon} - 0.43 \frac{\Gamma^2}{f}\right)^{2/3} \lesssim r_t \lesssim 1, \tag{6.12}$$

since the value of $r = \delta^{2/3} r_t$, obviously, must belong to the interval $z_\delta \lesssim r \lesssim \delta^{2/3}$, where z_δ is determined by (6.2). Finally, we have the estimation for the mean value (over the surface Σ_0) of the radial electric field $\langle E_r \rangle$ in the gas subdomain of the transition region:

$$\langle E_r(r_t) \rangle \equiv \frac{1}{\Sigma_0} \int_{\Sigma_0} (\boldsymbol{E} \cdot \boldsymbol{N}_0) \mathrm{d}\Sigma_0 = \frac{\delta^{-1/3} \Omega_0(r_t)}{2\pi(1 + \cos\alpha) r_t^2}. \tag{6.13}$$

Relations (5.35), (6.10)–(6.13) provide the electric field characteristics that could determine the production of gas phase ions due to their field evaporation inside the transition region.

7. Conclusions

In this paper, we have developed an asymptotic method of studying the structure of Taylor meniscus-jets. One limiting region in the space of parameters Ca, We, f, Mo, ϵ has been examined. It is described by conditions (4.6) and corresponds to sufficiently low flow rates of the liquid. The investigation of other regions of the parameter space is also of great importance. Some of them may describe the cone-jet mode with the cone semiangle less than $\alpha = 49.29°$. For example, such regimes are observed if $We \gg 1$ (Fernández de la Mora 1992). Other regions may not correspond to the cone-jet mode of electrospay atomization at all.

For the first time, we have obtained and studied the asymptotic solutions of the basic equations of electrohydrodynamics in all the outer subdomains (the meniscus, jet and surrounding gas), the gas solution having been matched with the jet and meniscus ones. This is the most important result of this paper from a theoretical point of view. The asymptotic method developed here has made it possible to obtain detailed information on the meniscus-jet structure. We have derived and analysed the following:

(i) distributions of the velocity, pressure, and electric potential inside the meniscus and jet;

(ii) the shape and surface charge of the meniscus and jet;

(iii) distribution of the electric field in the surrounding gas;

(iv) estimations of the electrohydrodynamic variables and liquid domain radius in the transition region.

It was found that the liquid density does not affect, to the leading order, the velocity, pressure, and electric potential inside the meniscus. However, it does affect the jet velocity, the surface charge and shape of the meniscus-jet, and the electric field in the surrounding gas. Surprisingly, the liquid viscosity affects no meniscus-jet or electric field characteristics, to the same order, except the velocity distribution inside the meniscus. This distribution is determined by the capillary number Ca and stream function $\psi(r, \theta)$ which are given by (1.5a) and (5.7a), Ca being proportional to the viscosity coefficient. The viscosity should be also important in the transition region V_t since the fluid dynamic equations in V_t are elliptic owing to the presence of viscosity. This feature is essential for the successful matching of outer and transition region expansions.

From a practical point of view, the most interesting characteristics of the cone-jet mode of electrospray atomization are those which can determine the production of charged drops and gas-phase ions. In this paper, we have found some of them using the asymptotic solutions obtained for all outer subdomains. We have derived relations (5.14), (5.15c), and (5.31b), which provide the velocity, charge, and radius of the jet. Subsequently we have calculated the electric field component normal to the meniscus-jet surface (see (5.33), (5.34), and (5.36)). Finally, we have estimated the electric field inside the transition region (see (5.35a) and (6.10)–(6.13)). The other essential result is a derivation of dependences (6.4) and (6.8) for the non-dimensional current $f(\epsilon)$. They are consistent with the scaling law (1.1) determined experimentally by Fernández de la Mora & Loscertales (1994) and data obtained by Chen & Pui (1997). In deriving (6.4) and (6.8), we have extrapolated the obtained asymptotic solutions into the transition region and then matched them in the limit $\delta \to 0$. To rigorously prove the scaling law (1.1), one should find an asymptotic solution to the basic equations of electrohydrodynamics in the transition region and match it with the solutions that have been obtained for the meniscus, jet and gas in § 5.

Comparing the theory with experiments, we should note the following important observations. Fernández de la Mora & Loscertales (1994) reported that they could not create the stable cone-jet mode at $\eta \lesssim 0.5$ which corresponds to $\delta \lesssim 10^{-2}$. That the asymptotic limit $\delta \to 0$ does not appear to be realized in experiments is not surprising, although the perturbation theory works at any small values of δ. This is a property of many asymptotic solutions in fluid mechanics. If a perturbation quantity is sufficiently close to its limit, new effects may arise and change the phenomenon in question to such an extent that it cannot be described by the original equations. A classical example is the impossibility of realizing a laminar boundary layer solution as the Reynolds number tends to infinity, due to the development of turbulence. However, asymptotic solutions are usually very useful in some region of small values of a perturbation quantity. Sometimes, they may continue to conform reasonably well to experimental data at values that are significant (Van Dyke 1975).

It is also worth noting that experiments are always carried out in a chamber of a finite size, and physical conditions at its walls are modelled by mathematical conditions at infinity. Such modelling can only be approximate as the meniscus and jet are assumed to stretch to infinity. For instance, in practical experiments, there might be an effect of the double layer charge at the inner surface of a capillary needle on a charge distribution in the meniscus. In sufficiently low-conductive liquids this double layer is not at equilibrium, and its charge can be swept downstream (Chernyi 1983). Obviously, this complication does not arise in the theoretical consideration of semi-infinite menisci. On the contrary, an ion distribution across the jet is not important since the terms caused by the ion mobility k_i and electrical conductivity K

(the terms with ϕ_0' in (3.10*a*)) vanish from the jet equations in the first approximation in δ (see (4.24*b*)).

I am grateful to Professor J. Fernández de la Mora (Yale University) who attracted my attention to the problems of electrospray atomization. His valuable comments have been greatly stimulating. I wish to thank the US National Science Foundation (Grant CTS-9319051) and a Goodyear grant from the State of Connecticut and Analytica of Branford for partial support of this effort.

Appendix. Stream function and pressure of the liquid flow inside the meniscus

Let us seek the solution to the problem (5.3)–(5.6) in the form

$$\psi = r^{1/2}\Psi(\theta), \quad P_1 = r^{-5/2}P(\theta). \tag{A 1a,b}$$

Substituting (A 1) into (5.3)–(5.6), we obtain equations to determine Ψ and P:

$$\hat{\mathrm{D}}_{-3/2}\hat{\mathrm{D}}_{1/2}\Psi = 0 \quad \left(\hat{\mathrm{D}}_v \equiv v(v-1) + \sin\theta\frac{\mathrm{d}}{\mathrm{d}\theta}\frac{1}{\sin\theta}\frac{\mathrm{d}}{\mathrm{d}\theta}\right), \tag{A 2}$$

$$P = \frac{2}{5\sin\theta}\frac{\mathrm{d}\hat{\mathrm{D}}_{1/2}\Psi}{\mathrm{d}\theta}, \quad \frac{\mathrm{d}P}{\mathrm{d}\theta} = -\frac{3\hat{\mathrm{D}}_{1/2}\Psi}{2\sin\theta}, \tag{A 3a,b}$$

and the boundary conditions to them:

$$\Psi = 0, \quad \frac{\mathrm{d}}{\mathrm{d}\theta}\frac{1}{\sin\theta}\frac{\mathrm{d}\Psi}{\mathrm{d}\theta} = Bf \quad \text{at} \quad \theta = \alpha, \tag{A 4a,b}$$

$$\Psi = 0, \quad \frac{\mathrm{d}\Psi}{\mathrm{d}\theta} = 0 \quad \text{at} \quad \theta = 0. \tag{A 5a,b}$$

It should be observed that equation (A 3*b*), which has resulted from (5.4*b*), is not independent of relations (A 3*a*), (A 2) and therefore can be dropped. Indeed, substitution of (A 3*a*) into (A 3*b*) yields (A 2).

Since the operators $\hat{\mathrm{D}}_{1/2}$ and $\hat{\mathrm{D}}_{-3/2}$ are commutative, a general solution to the problem (A 2), (A 5) is given by

$$\Psi = g_1 G_{1/2}(\cos\theta) + g_2 G_{-3/2}(\cos\theta), \tag{A 6}$$

where g_1 and g_2 are arbitrary constants, $G_{1/2}(\cos\theta)$ and $G_{-3/2}(\cos\theta)$ are regular (at $\theta = 0$) solutions to the Gegenbauer equations:

$$\hat{\mathrm{D}}_{1/2}G_{1/2} = 0, \quad \hat{\mathrm{D}}_{-3/2}G_{-3/2} = 0. \tag{A 7a,b}$$

They can be represented as (Kamke 1942)

$$G_{1/2} = -\sin\theta P'_{-1/2}(\cos\theta), \quad G_{-3/2} = -\sin\theta P'_{3/2}(\cos\theta), \tag{A 8a,b}$$

where $P_{-1/2}$ and $P_{3/2}$ are the standard Legendre functions of degree $-1/2$ and $3/2$, respectively, and primes denote the derivatives with respect to θ. Substituting (A 8) into (A 6) and, in turn, (A 6) into (A 4) and taking into account the fact that the functions $G_{1/2}$ and $G_{-3/2}$ satisfy (A 7), we obtain the system of two linear algebraic

equations for g_1 and g_2:

$$g_1 P'_{-1/2}(\cos\alpha) + g_2 P'_{3/2}(\cos\alpha) = 0, \tag{A 9a}$$

$$g_1 P'_{-1/2}(\cos\alpha) - 15 g_2 P'_{3/2}(\cos\alpha) = -4Bf, \tag{A 9b}$$

which yield

$$g_1 = -\frac{Bf}{4P'_{-1/2}(\cos\alpha)}, \quad g_2 = \frac{Bf}{4P'_{3/2}(\cos\alpha)}. \tag{A 10a,b}$$

Substituting (A 8) and (A 10) into (A 6), we obtain the function $\Psi(\theta)$ which appears in expression (A 1 *a*) for the stream function $\psi(r,\theta)$:

$$\Psi = \frac{Bf\sin\theta}{4}\left(\frac{P'_{-1/2}(\cos\theta)}{P'_{-1/2}(\cos\alpha)} - \frac{P'_{3/2}(\cos\theta)}{P'_{3/2}(\cos\alpha)}\right). \tag{A 11}$$

Finally, substitution of (A 11) into (A 3*a*) yields the function $P(\theta)$ which appears in expression (A 1*b*) for the leading term of the (scaled) liquid pressure P_1 inside the meniscus:

$$P = -\frac{3BfP_{3/2}(\cos\theta)}{2P'_{3/2}(\cos\alpha)}. \tag{A 12}$$

Using (5.2), (A 1), (A 11), and (A 12), we also find the leading terms of the (scaled) velocity components inside the meniscus:

$$U_{1r} = -\frac{fW(\theta)}{r^{3/2}}, \quad U_{1\theta} = \frac{\Psi(\theta)}{2r^{3/2}\sin\theta}, \tag{A 13a,b}$$

and the leading term of the (scaled) normal liquid stress at the meniscus surface:

$$-\left(P_1 - 2\boldsymbol{n}\cdot\frac{\mathrm{d}\boldsymbol{U}_1}{\mathrm{d}n}\right)_{\theta=\alpha} = \frac{-1}{r^{5/2}}\left(P(\alpha) + \frac{\Psi'(\alpha)}{\sin\alpha}\right) = \frac{-Cf}{r^{5/2}}, \tag{A 14}$$

where

$$W(\theta) \equiv \frac{B}{16}\left(\frac{P_{-1/2}(\cos\theta)}{P'_{-1/2}(\cos\alpha)} + 15\frac{P_{3/2}(\cos\theta)}{P'_{3/2}(\cos\alpha)}\right), \tag{A 15}$$

$$C = \frac{B}{16}\left(\frac{P_{-1/2}(\cos\alpha)}{P'_{-1/2}(\cos\alpha)} - 9\frac{P_{3/2}(\cos\alpha)}{P'_{3/2}(\cos\alpha)}\right) = 0.45, \tag{A 16}$$

and the constant B is defined by (5.5). In particular, (A 15) yields

$$W(\alpha) = 0.146, \quad W(0) = -0.154. \tag{A 17}$$

Substituting (A 13*a*) and (5.8*a*) into the asymptotic expansion (4.1) for the liquid velocity $\boldsymbol{u}$ and making use of (A 17), we obtain expressions (5.9) for $\boldsymbol{u}$. Finally, relation (A 14) allows us to readily calculate the left-hand side of the boundary condition (4.15) which determines the meniscus surface perturbation.

REFERENCES

Abramovitz, M. & Stegun, I. A. 1964 *Handbook of Mathematical Functions*. Washington: National Bureau of Standards.

Anno, J. N. 1977 *The Mechanics of Liquid Jets*. Lexington Books.

Bailey, A. G. 1988 *Electrostatic Spraying of Liquids*. Wiley.

Benasayag, G. & Sudraud, P. 1985 In situ high voltage TEM observations of an EHD source. *Ultramicroscopy* **16**, 1–8.

Chen, D.-R. & Pui, D. Y. H. 1997 Experimental investigation of scaling laws for electrospraying: dielectric constant effect. *Aerosol Sci. Technol.* **27**, 367–380.

Chen, D.-R., Pui, D. Y. H. & Kaufman, S. L. 1995 Electrospraying of conducting liquids for monodisperse aerosol generation in the 4 nm to 1.8 μm diameter range. *J. Aerosol Sci.* **26**, 963–977.

Chernyi, L. T. 1983 Electrohydrodynamic models and methods for calculating the electrification of organic liquids flowing in pipes. *Sov. Phys. Dokl.* **28**, 539–541.

Cloupeau, M. & Prunet-Foch, B. 1989 Electrostatic spraying of liquids in cone-jet mode. *J. Electrostat.* **22**, 135–159.

Cloupeau, M. & Prunet-Foch, B. 1990 Electrostatic spraying of liquids: main functioning modes. *J. Electrostat.* **25**, 165–184.

Cloupeau, M. & Prunet-Foch, B. 1994 Electrohydrodynamic spraying functioning modes: a critical review. *J. Aerosol Sci.* **25**, 1021–1036.

Dubrovin, B. A., Fomenko, A. T. & Novikov, S. P. 1984 *Modern Geometry – Methods and Applications. Part I. The Geometry of Surfaces, Transformation Groups, and Fields.* Springer.

Eggers, J. 1995 Theory of drop formation. *Phys. Fluids* **7**, 941–953.

Eggers, J. & Dupont, T. F. 1994 Drop formation in a one-dimensional approximation of the Navier–Stokes equation. *J. Fluid Mech.* **262**, 205–221.

Fenn, J. B., Mann, M., Meng, C. K., Wong, S. F. & Whitehouse, C. M. 1989 Electrospray ionization for mass spectrometry of large biomolecules. *Science* **246**, 64–71.

Fernández de la Mora, J. 1992 The effect of charge emission from electrified liquid cones. *J. Fluid Mech.* **243**, 561–574.

Fernández de la Mora, J. 1996 On the outcome of the Coulombic fission of a charged isolated drop. *J. Colloid Interface Sci.* **178**, 209–218.

Fernández de la Mora, J. & Loscertales, I. G. 1994 The current emitted by highly conducting Taylor cones. *J. Fluid Mech.* **260**, 155–184.

Gabovich, M. D. 1984 Liquid-metal emitters. *Sov. Phys. Usp.* **26**, 447–455.

Gañán-Calvo, A. M. 1997*a* On the theory of electrohydrodynamically driven capillary jets. *J. Fluid Mech.* **335**, 165–188.

Gañán-Calvo, A. M. 1997*b* Cone-jet analytical extension of Taylor's electrostatic solution and the asymptotic universal scaling laws in electrospraying. *Phys. Rev. Lett.* **79**, 217–220.

Gañán-Calvo, A. M., Dávila, J. & Barrero, A. 1997 Current and droplet size in the electrospraying of liquids. Scaling laws. *J. Aerosol Sci.* **28**, 249–275.

Gleiter, H. 1989 Nanocrystalline materials. *Prog. Mater. Sci.* **33**, 223–315.

Gomez, A. & Tang, K. 1994 Charge and fission of droplets in electrostatic sprays. *Phys. Fluids* **6**, 404–414.

Grace, J. M. & Marijnissen, J. C. M. 1994 A review of liquid atomization by electrical means. *J. Aerosol Sci.* **25**, 1005–1019.

Gutmanas, E. Y. 1990 Materials with fine microstructures by advanced powder metallurgy. *Prog. Mater. Sci.* **34**, 261–366.

Happel, J. & Brenner, H. 1965 *Low Reynolds Number Hydrodynamics with Special Applications to Particulate Media.* Prentice-Hall.

Hayati, I., Bailey, A. I. & Tadros, Th. F. 1986 Mechanism of stable jet formation in electrohydrodynamic atomization. *Nature* **319**, 41–43.

Hayati, I., Bailey, A. I. & Tadros, Th. F. 1987 Investigations into the mechanism of electrohydrodynamic spraying of liquids. II Mechanism of stable jet formation and electrical forces acting on a liquid cone. *J. Colloid Interface Sci.* **117**, 222–230.

Joffre, G.-H. & Cloupeau, M. 1986 Characteristic forms of electrified menisci emitting charges. *J. Electrostat.* **18**, 147–161.

Jones, A. R. & Thong, K. C. 1971 The production of charged monodisperse fuel droplets by electrostatic dispersion. *J. Phys.* D: *Appl. Phys.* **4**, 1159–1166.

Kamke, E. 1942 *Differentialgleichungen, Lösungsmethoden und Lösungen.* Akademische Verlagsgesellschaft, Leipzig.

Lohmann, M. & Schmidt-Ott, A. 1995 Production of metallic nanoparticles via electrostatic atomization. *J. Aerosol Sci.* **26**, S829–S830.

Melcher, J. R. & Warren, E. P. 1971 Electrohydrodynamics of a current-carrying semi-insulating jet. *J. Fluid Mech.* **47**, 127–143.

Mestel, A. J. 1994*a* The electrohydrodynamic cone-jet at high Reynolds number. *J. Aerosol Sci.* **25**, 1037–1047.

Mestel, A. J. 1994*b* Electrohydrodynamic stability of a slightly viscous jet. *J. Fluid Mech.* **274**, 93–113.

Mestel, A. J. 1996 Electrohydrodynamic stability of a highly viscous jet. *J. Fluid Mech.* **312**, 311–326.

Pantano, C., Gañán-Calvo, A. M. & Barrero, A. 1994 Zeroth-order, electrohydrostatic solution for electrospraying in cone-jet mode. *J. Aerosol Sci.* **25**, 1065–1077.

Papageorgiou, D. T. 1995*a* On the breakup of viscous liquid threads. *Phys. Fluids* **7**, 1529–1544.

Papageorgiou, D. T. 1995*b* Analytical description of the breakup of liquid jets. *J. Fluid Mech.* **301**, 109–132.

Rosell-Llompart, J. & Fernández de la Mora, J. 1994 Generation of monodisperse droplets 0.3 to 4 μm in diameter from electrified cone-jets of highly conducting and viscous liquids. *J. Aerosol Sci.* **25**, 1093–1119.

Scriven, L. E. 1960 Dynamics of a fluid interface. Equation of motion for Newtonian surface fluids. *Chem. Engng Sci.* **12**, 98–108.

Shtern, V. & Barrero, A. 1994 Striking features of fluid flows in Taylor cones related to electrosprays. *J. Aerosol Sci.* **25**, 1049–1063.

Shtern, V. & Barrero, A. 1995 Bifurcation of swirl in liquid cones. *J. Fluid Mech.* **300**, 169–205.

Smith, R. D., Loo, J. A., Ogorzalek Loo, R. R., Busman, M. & Udseth, H. R. 1991 Principles and practice of electrospray ionization – mass spectrometry for large polypeptides and proteins. *Mass Spectrom. Rev.* **10**, 359–451.

Tang, K. & Gomez, A. 1994 Generation by electrospray of monodisperse water droplets for targeted drug delivery by inhalation. *J. Aerosol Sci.* **25**, 1237–1249.

Taylor, G. I. 1964 Disintegration of water drops in an electric field. *Proc. R. Soc. Lond.* **A 280**, 383–397.

Van Dyke, M. 1975 *Perturbation Methods in Fluid Mechanics.* The Parabolic Press.

Zeleny, J. 1914 The electrical discharge from liquid points and a hydrostatic method of measuring the electric intensity at their surface. *Phys. Rev.* **3**, 69–91.

Zeleny, J. 1917 Instability of electrified liquid surfaces. *Phys. Rev.* **10**, 1–6.